FINAL REPORT

Improved Understanding of In Situ Chemical Oxidation Contaminant Oxidation Kinetics

SERDP Project ER-1289

December 2007

Paul Tratnyek
Oregon Health & Science University

Jamie Powell
Oregon Health & Science University

Rachel Waldemer
Oregon Health & Science University

IMPROVED UNDERSTANDING OF IN SITU CHEMICAL OXIDATION
Technical Objective I: Contaminant Oxidation Kinetics

SERDP Project Number ER-1289

Principal Investigator: Paul G. Tratnyek

Graduate Students and Staff: Rachel Waldemer and Jamie Powell

Department of Environmental and Biomolecular Systems

Oregon Health & Science University

20000 NW Walker Rd., Beaverton, OR 97006-8921

*Email: tratnyek@ebs.ogi.edu

Web: http://cgr.ebs.ogi.edu

Phone: 503-748-1023, Fax: 503-748-1273

FINAL REPORT—OBJECTIVE I

May 2009

Revision 1

TABLE OF CONTENTS

LIST of TABLES

LIST of FIGURES

LIST of FIGURES, cont.

LIST of ACRONYMS

A	pre-exponential factor
BTEX	benzene, toluene, xylene
ºC	degrees Celcius
$CHCl_3$	chloroform
$Cl^{\bullet}$	chlorine radical
COC	contaminant of concern
DCE	1,1-dichloroethene
DDT	1,1,1-trichloro-2,2-bis(p-chlorophenyl)ethane
$E_{1/2}$	half-wave potential
E_A	apparent activation energy
E_{GAP}	the energy difference between the HOMO and the LUMO
E_{HOMO}	energy of the highest occupied molecular orbital
H_2O_2	hydrogen peroxide
HMX	cyclotetramethylene-tetranitramine
HOMO	highest occupied molecular orbital
IP	ionization potential
ISCO	in situ chemical oxidation
ISCOKIN	database containing our collection of k'' data
ISTR	in situ thermal remediation
k_{obs} or k'	pseudo-first-order rate constants
k''	second-order rate constants
LUMO	lowest unoccupied molecular orbital
M	molar
mg/L	milligrams per liter
mM	millimolar
MnO_4^-	permanganate
MnO_2	manganese dioxide
MTBE	methyl tert butyl ether
NAPL	non-aqueous phase liquid
NOD	natural oxidant demand
•OH	hydroxide radical
Ox	oxidant
O_3	ozone
PCE	perchloroethylene
HSO_5^-	peroxymonosulfate
PNDA	p-nitrosodimethylaniline
QSARs	quantitative structure-activity relationships
R	universal gas constant
RDX	cyclotrimethylenetrinitramine
$S_2O_8^{2-}$	Persulfate
$SO_4^{\bullet-}$	sulfate radical
T	absolute temperature
TCE	trichloroethylene
TNT	trinitrotoluene

1. Acknowledgements

The majority of the experimental work, and much of the data mining and literature analysis that comprised this project was performed by Rachel H. Waldemer. Additional contributions were made by Jamie S. Powell and James T. Nurmi. Richard L. Johnson contributed to the work on activated persulfate. We thank Eric Hood and Neil Thomson for helpful comments on some of documents on permanganate.

2. Executive Summary

The overall goal of Technical Objective 1: Contaminant Oxidation Kinetics for this project was to provide a comprehensive perspective on the kinetics of oxidation of groundwater contaminants by ISCO oxidants. We did this by summarizing previously published (second order) rate constants for all of the putative oxidants (mainly permanganate anion, hydroxyl radical, and sulfate radical). Where important data gaps are discovered, we measured rate constants in the laboratory. The overall dataset was used to develop quantitative structure-activity relationships (QSARs) for predicting rate constants were none have been measured.

First, we developed a novel method for measuring rate constants of contaminant oxidation by permanganate. Permanganate disappearance kinetics are pseudo-first-order as long as contaminant concentrations are in excess. The colloidal manganese dioxide that forms from permanganate oxidation gives Beer's law behavior, and a procedure was developed to correct for any interference this caused.

Using this method, the oxidation of most contaminants by permanganate was shown to be first-order in contaminant concentration (second-order overall) by varying initial concentrations of contaminant. The second-order rate constants obtained with our method are in good agreement with those previously reported values for perchloroethylene (PCE) and trichloroethylene (TCE). Further measurements with a chlorinated ethane (1,1,1-trichloroethane) and a BTEX constituent (toluene) show that reaction of these contaminants with permanganate is slow. Other classes of contaminants that were tested include chlorinated methanes (carbon tetrachloride, etc.), explosives (TNT, RDX), and oxygenates (MTBE).

Activated persulfate produces sulfate radical, hydroxyl radicals, and other reactive intermediates. We investigated three methods for activation of persulfate (light, heat, and chelated ferrous iron) and showed that these methods produced very different amounts of radical intermediates. We developed a method for measuring rate constants for contaminant oxidation

by sulfate radical and applied it to a variety of contaminants including the BTEX compounds, chlorinated methanes, 1,4-dioxane, and MTBE. Rate constants for reactions with sulfate radical were related to rate constants for hydroxyl radical to shed some light on the relative significance of these two oxidants during ISCO with activated persulfate (under laboratory and field conditions).

While chlorinated ethenes have been successfully remediated with both in situ chemical oxidation (ISCO) and in situ thermal remediation (ISTR), there is evidence that combining these two treatment approaches may result in synergistic advantages. Sodium persulfate is an ideal oxidant for combination with ISTR because persulfate exposure to high temperatures leads to the formation of highly reactive sulfate radicals in addition to the higher reaction rates normally induced by higher temperatures. We have found that the reactions of chlorinated ethenes and heat-activated sodium persulfate are first-order with respect to chlorinated ethenes for at least the first one to two half-lives, and with sodium persulfate in excess, the resulting pseudo-first-order reactions can be described by the Arrhenius equation. The dichloroethenes appear to mineralize more completely than TCE and PCE based on chlorine recovery analysis.

Using Arrhenius parameters (both published and those determined here) for permanganate oxidation, persulfate oxidation, and hydrolysis (the ubiquitous degradation process that could be significant at higher temperatures), comparisons for these three degradation processes were made over the temperature range of 0 to 100 C. It was determined that hydrolysis is never important for the chlorinated ethenes. For PCE, permanganate oxidation may be more favorable at lower temperatures, but persulfate oxidation is more favorable at higher temperature.

In situ chemical oxidation of chlorinated solvents with activated persulfate has received considerable study in the last few years, with much of this work focused on comparison of alternative methods for activation (heat, iron, peroxide, etc.). By comparison, data on the oxidation of other contaminants by activated persulfate are relatively scarce. We revisited the oxidation of explosives with heat-activated persulfate and found fairly rapid degradation of TNT, RDX, HMX, and 4-nitrophenol. The kinetics generally are first-order and the effect of temperature follows the Arrhenius model. The reaction mechanism probably is not dominated by electron-transfer to sulfate radical—as is the case with most organic oxidations by activated persulfate—because the explosives are very poor electron donors. Instead the reaction presumably involves sulfate radical addition or substitution, but this cannot yet be confirmed because no products have been identified to date.

3. Project Objectives

The use of in situ chemical oxidation (ISCO) for treatment of chlorinated solvent source areas is rapidly increasing as Department of Defense (DoD) and other stakeholders search for remedial approaches that reduce long-term operations and maintenance requirements. While ISCO is a promising technology for some chemicals, there remains significant data needs related to: i) reaction kinetics for common DoD contaminants; ii) the effects of natural oxidant demand on oxidant mobility and delivery under varying site conditions; and iii) the effects of ISCO on long-term groundwater quality. This study, Strategic Environmental Research and Development Program (SERDP) research project CU-1289 (An Improved Understanding of In Situ Chemical Oxidation), focused on addressing these data needs for permanganate, persulfate and Fenton's reagent. The overall goal of this research program was to address critical research needs for the improved implementation of ISCO using Fenton's reagent, persulfate or permanganate. These critical research needs include: Technical Objective 1, the development of a comprehensive kinetic perspective on the kinetics of oxidation of common DoD contaminants by the most commonly used oxidants, permanganate (MnO_4^-), Fenton's reagent (H_2O_2/Fe^{2+}) and persulfate; and Technical Objective 2, assess how soil properties (e.g., soil mineralogy, natural carbon content) affect oxidant mobility and stability in the subsurface, and develop a standardized natural oxidant demand (NOD) measurement protocol.

This project report is divided into two Final Reports that address each of these critical research needs: Contaminant Oxidation Kinetics and Soil Reactivity. This Final Report addresses Contaminant Oxidation Kinetics and was completed by the Oregon Health and Sciences University. The Final Report for Soil Reactivity was completed by the University of Waterloo. These reports build upon the research results previously presented in this project's 2003 and 2004 Annual Reports submitted to SERDP (Geosyntec, OHSU, and UW, 2003 and 2005).

4. Overview

In the last few years, a few detailed studies have been reported on the kinetics and mechanism by which permanganate oxidizes key groundwater contaminants, mainly the chlorinated ethenes (Huang et al., 1999; Hood et al., 2000; Yan and Schwartz, 2000). The literature on oxidation of organics by Fenton's reagent is considerably larger, but even there, the scope of most detailed studies of kinetics and mechanisms tends to be narrow with respect to the number and type of contaminants considered (e.g., Lipczynska-Kochany, 1991; Sedlak and Andren, 1991; Leung et al., 1992; Huston and Pignatello, 1996; Li et al., 1997; Tang and Tassos, 1997; Augusti et al., 1998; Bier et al., 1999). A distinguishing feature of this project was that it

focused on identifying the kinetic and mechanistic characteristics that are common to a range of contaminant oxidation reactions, with the ultimate goal of producing a comprehensive perspective on the chemistry of ISCO technologies.

The lack of a comprehensive perspective on the chemistry of ISCO technologies is evident from the numerous inconsistencies in how oxidation by permanganate or Fenton's reagant are treated by most environmental chemists and engineers. For example, the strength of both oxidants is frequently equated with their very positive oxidation potentials by advocates of ISCO technologies, even though it is unusual for either oxidant to react by electron transfer (Tratnyek and Macalady, 2000). For permanganate, the only detailed mechanism for oxidation of organics that has been described in the environmental literature involves electrophilic addition and rearrangement of chlorinated ethenes (Yan and Schwartz, 2000). But even this may not be the whole story, as recent evidence in the chemical literature has shown that permanganate reacts with most organics by hydride abstraction (Gardner and Mayer, 1995; Mayer, 1998).

With respect to groundwater applications of activated hydrogen peroxide processes (i.e., the Fenton reaction), similar inconsistencies exist. For example, it is almost universally assumed that oxidation is mediated by hydroxyl radical, even though there is still a raging debate in the chemical literature regarding the relative importance of hydroxyl radical vs. other intermediates in activated hydrogen peroxide systems (Sawyer et al., 1996; MacFaul et al., 1998; Walling, 1998; Goldstein and Meyerstein, 1999). Remarkably, the reactive intermediates other than hydroxyl radical that have received the most attention in the environmental literature are superoxide and hydroperoxide anion (Watts et al., 1999), and these species are hardly mentioned in the debate on this topic among the chemists. Clearly, there still is considerable uncertainty over how activated hydrogen peroxide degrades organic substance in water, despite many years of research in this area.

Despite these uncertainties in the mechanism of contaminant degradation by permanganate and Fenton's reagent, some very complex and detailed kinetic models have been described for these oxidants (e.g., Hong et al., 1996; Yan and Schwartz, 2000; Zhang and Schwartz, 2000). The development and application of these models has advanced our understanding of advanced oxidation processes considerably, but they have rarely been applied directly to the design ISCO applications in the field by practitioners of these technologies. Another goal of this project is to bridge the gap between the most detailed kinetics models and the highly simplified kinetic models that are (often implicitly) used in engineering design.

The philosophy that we bring to this problem is exemplified in the influential work of Prof. Jürg Hoigné and coworkers for describing the kinetics of contaminant oxidation in disinfection

and photolysis (e.g., Hoigné and Bader, 1983a; Hoigné, 1990; Tratnyek and Hoigné, 1991; Hoigné and Bader, 1993). The approach is basically to focus on parameterizing the model as the sum of independent second-order rate laws involving measurable reactant concentrations. Although there is nothing novel about this approach per se, a significant challenge lies in codifying this process at a level that is rigorous (in a physical chemical sense) and yet still applicable to complex, real-world situations. One way to do this is summarized in Figure 1.

The approach taken in this project was primarily to proceed from the top of Figure 1 to the bottom, via equations 1-4, in order to derive generally-useful properties of each combination of a contaminant of concern (COC) and oxidant (Ox). This is relatively straight forward with permanganate because experiments with permanganate are formulated with the oxidant in excess, such that [Ox] is known and constant. In contrast, with activated hydrogen peroxide the primary oxidant is hydroxyl radical (•OH), which is a reactive intermediate that is generated at a very low but steady state concentration (thus the subscript "ss"). A similar situation exists with activated persulfate, where the primary oxidant is sulfate radical ($SO_4^{\bullet-}$). Note that other experimental variables can be accommodated in this scheme, if necessary. Most notably, temperature can be described by inserting the Arrhenius equation between equations 2 and 4. Once the fundamental kinetic data (second order rate constants, k'') are available, Figure 1 can be applied from the bottom up by practitioners to estimate the performance of a ISCO treatment under a particular set of conditions.

In light of the importance of good kinetic data, we compiled the values of k'' from the literature for oxidation of a variety of contaminants by permanganate (MnO_4^-); hydroxyl radical (•OH), often thought to be the reactive species formed by the Fenton reaction (Pignatello et al., 2006); and sulfate radical ($SO_4^{\bullet-}$), thought to be the reactive species formed by activated persulfate (Kolthoff et al., 1951; Peyton, 1993; Couttenye et al., 2002). We then determined the priority data gaps, designed several methods for filling the data gaps for these oxidants, and applied these methods to many priority COCs (focusing on emerging contaminants, contaminants that are prevalent at military sites, and contaminants that form non-aqueous

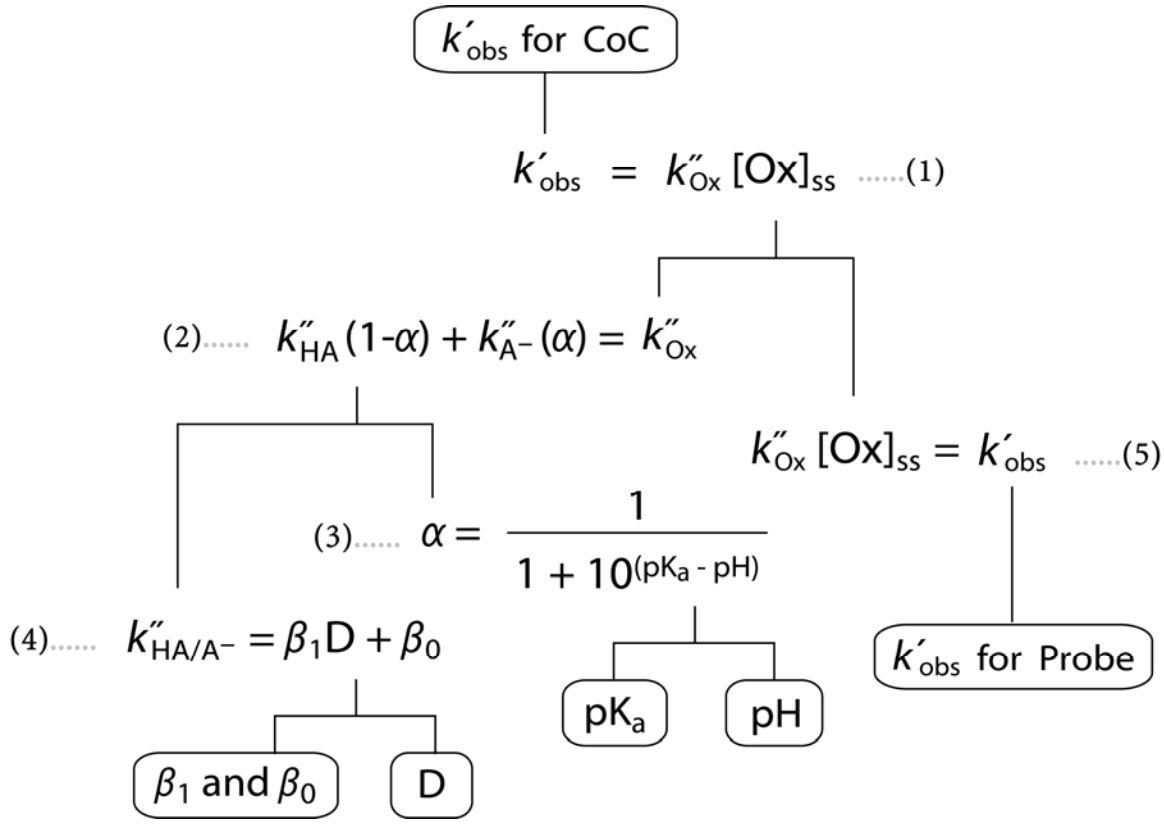

Figure 21. General scheme summarizing how to represent the disappearance kinetics of a contaminant of concern (COC) due to reaction with an oxidant (Ox). Pseudo first order rate constants (*k′*) are used to describe the kinetics of a particular reaction under specific conditions, from which second-order rate constants (*k″*) are derived to characterize the reaction in general. The effect of pH is shown where it involves speciation of the COC into protonated and deprotonated forms (HA and A^-), but an analogous treatment is possible if pH effects are due to speciation of the Ox. QSARs that can predict *k″* can be expressed as linear models with one or several descriptor variables (D) and the associated slopes and intercept (β_1 and β_0). A probe substance can be used to determine the steady-state (ss) concentration of intermediate oxidants such as hydroxyl radical.

phase liquids in the environment). Then, combining new and previously published data for *k″*, we performed correlation analysis to: (*i*) assess the overall quality of the data set, (*ii*) investigate the possibility that quantitative structure-activity relationships (QSARs) could be developed to predict values of *k″* for COCs that have not been studied, and (*iii*) examine whether the different oxidants showed similar patterns of reactivity with the same set of contaminants, indicating whether different oxidants had similar mechanisms of reactivity.

While most of our research for this project focused on compiling and generating new values of *k″*, there were some situations—mainly involving activated peroxide and persulfate—

for which it was more practical to focus on pseudo-first-order rate constants (k_{obs} or k'). For example, this was the case when we were studying the effects of temperature on the oxidation of chlorinated ethenes by heat-activated persulfate (Section 11). Using k_{obs} as our kinetic parameter allowed us to measure the global effect of temperature on the many reactions that are generated once persulfate is activated. While this is a less rigorous approach, studying the effect of temperature on each reaction would be a lengthy process and was not possible within the time-scale of the study; furthermore, it is not likely that the detail gained from this approach would change the conclusions that were drawn by using k_{obs}.

5. Outline of Tasks

The kinetics part of this project was structured in six tasks: (*i*) assemble and summarize existing kinetic data, (*ii*) determine and prioritize key data gaps, (*iii*) validate a novel experimental method for measuring new kinetic data, (*iv*) apply our experimental method to fill the most important data gaps, (*v*) perform correlation analysis on new and old data together to validate them all and derive models that can predict data that are unavailable, and (*vi*) begin calibration of a quantitative kinetic that can describe the effect of competition among multiple oxidants. Tasks 1-4 apply separately to permanganate, activated peroxide, and activated persulfate, whereas Tasks 5-6 apply to all the ISCO chemistries collectively.

Task 1. A exhaustive literature review was conducted for previously published kinetic data on the oxidation of NAPL constituents by permanganate, hydroxyl radical, and sulfate radical. The results of this work have been (or will be) published in print and online, and are incorporated in Sections 6, 8, 9, and 11 as well as in the ISCOKIN database (Section 10).

Task 2. To identify and prioritize key data gaps, we summarized the data from Task 1 into a variety of formats. Figures and tables of these results were presented at various meetings and the first annual report for this project. Beyond that, they have not been published because there purpose is largely help with prioritization of the work on the tasks that follow.

Task 3. In preparation for experimental work to fill some of the data gaps identified in Task 2, we investigated, evaluated, and validated a variety of experimental approaches: (*i*) serial sampling of shaken bottles (Tratnyek, 1998; Hood et al., 2000; Yan and Schwartz, 2000), (*ii*) serial sampling and continuous monitoring of stirred reactors (Yan and Schwartz, 1999), (*iii*) serial sampling of a stirred syringe reactor (Huang et al., 1999), and (*iv*) continuous monitoring with a stopped flow reactor (Nam and Tratnyek, unpublished data). Different methods were used for different oxidants, so they are described below together with the results for each oxidant.

Task 4. Using the methods developed under in Task 3, we measured new values of k'' for permanganate and activated persulfate but not activated peroxide (because the existing data for •OH reaction with organic contaminants is very extensive and extraction of k'' from data for Fe(II) activated peroxide would have been very complex and time consuming). For permanganate and activated persulfate, we determined how the kinetics of contaminant oxidation were affected by key experimental variables (e.g., temperature and pH). These results are described in Sections 6-8, 11-12.

Task 5. The combination of new kinetic data from Task 4 and previously published kinetic data from Tasks 1-2 were subjected to a comprehensive "correlation analysis" (Tratnyek, 1998; Farrell and Luo, 2002). Correlation analysis is a very powerful tool for two more specific ends: (*i*) verification that the data are free of erroneous or inconsistent values, and (*ii*) derivation of quantitative structure-activity relationships (QSARs) for predicting data that are not available. The results of this are summarized in Section 9; they have not yet been published but we expect they will be once we have found time to resolve several residual issues with this analysis.

Task 6. Although the kinetic scheme set out in Figure 1 should be sufficient to characterize the major "intrinsic" factors that determine the kinetics of oxidation in solution, there are a host of environmental factors that may decrease the rate of contaminant oxidation through competition for the oxidant. These competitors for oxidant can be other organic contaminants, natural organic matter, various inorganic solutes like carbonate, and mineral surfaces. We performed experiments to characterize the competitive effect of the most important of these groundwater constituents, and the results are included below in Section 12.

6. Determining k" for Permanganate[1,2,3]

To measure *k"* for contaminant oxidation by permanganate, we used absorbance spectrometry, an efficient method that allowed us to measure the kinetics of oxidation for 24 contaminants—many for which data were not previously available. A factor that complicates the use of absorbance spectrometry to follow oxidation reactions involving MnO_4^- is that the reduction product, colloidal MnO_2, contributes to the absorbance measured at 525 nm (an absorbance maximum for MnO_4^-) (Mata-Perez and Perez-Benito, 1985; Perez-Benito and Arias, 1992; Gardner, 1996; Yan and Schwartz, 1999). Fortunately, the measured absorbance of colloidal MnO_2 suspensions obeys Beer's Law until the particles begin to flocculate, resulting in increased scattering of light by the larger aggregates (Mata-Perez and Perez-Benito, 1985; Perez-Benito and Arias, 1992). Our methods to determine where Beer's Law was obeyed in our system are discussed elsewhere (Waldemer, 2004; Waldemer and Tratnyek, 2004; Waldemer and Tratnyek, 2006).

After excluding the data where scattering by colloidal MnO_2 was significant (causing deviation from Beer's Law), we found that most COCs gave data for absorbance at 525 nm vs. time that fit pseudo-first-order kinetics with a modest deviation from this kinetic model as the reaction approached completion (Figure 2). We concluded that the latter effect was due to increasing light absorption by suspended MnO_2, based on comparison with previously published spectra for colloidal MnO_2 suspensions (Perez-Benito and Arias, 1992). To obtain pseudo-first-order rate constants (k_{obs}) in a manner that systematically accounts for the absorbance of colloidal MnO_2, we fit all of our kinetic data to a two-term model:

$$A_{525} = [C_i e^{-k_{obs}t}] \times \varepsilon_{MnO_4^-}^{525} + [C_i - C_i e^{-k_{obs}t}] \times \varepsilon_{MnO_2}^{525} \qquad [6]$$

---

[1] Waldemer, R. H.; Tratnyek, P.G. (2006) Kinetics of contaminant degradation by permanganate. *Environ. Sci. Technol.* 40(3): 1055-1061.

[2] Waldemer, R. H.; Tratnyek, P.G. (2004) The efficient determination of rate constants for oxidations by permanganate. *Proceedings of the Fourth International Conference on Remediation of Chlorinated and Recalcitrant Compounds, 24-27 May 2004,* Monterey, CA, Paper 2A-09.

[3] Waldemer, R. H. (2004) Determination of the Rate of Contaminant Degradation by Permanganate: Implications for In Situ Chemical Oxidation (ISCO). M.S. thesis, OGI School of Science and Engineering, Portland, OR.

where A_{525} is the absorbance at 525 nm, C_i is the initial amount of MnO_4^-, $\varepsilon_{MnO_4^-}^{525}$ is the absorptivity of MnO_4^-, and $\varepsilon_{MnO_2}^{525}$ is the absorptivity of MnO_2. We treated C_i and $\varepsilon_{MnO_4^-}^{525}$ as constants and simultaneously fit k_{obs} and $\varepsilon_{MnO_2}^{525}$ by least squares regression. This treatment allows for variability in $\varepsilon_{MnO_2}^{525}$, which is expected because the optical properties of the particles will depend on their size distribution, and which will be affected by the rate of MnO_4^- reduction, which will depend on the COC that is being oxidized. The fitted values we obtained for $\varepsilon_{MnO_2}^{525}$ have a roughly normal distribution (statistical analysis given in (Waldemer, 2004)). Overall, equation 6 fit the experimental data very well, as illustrated in Figure 2A for a fast reaction (3-chlorophenol, with a half-life of seconds) and Figure 2B for a slow reaction (1,4-dioxane, with a half-life of days). Further details on the derivation and validation of equation 6 can be found in (Waldemer, 2004; Waldemer and Tratnyek, 2004).

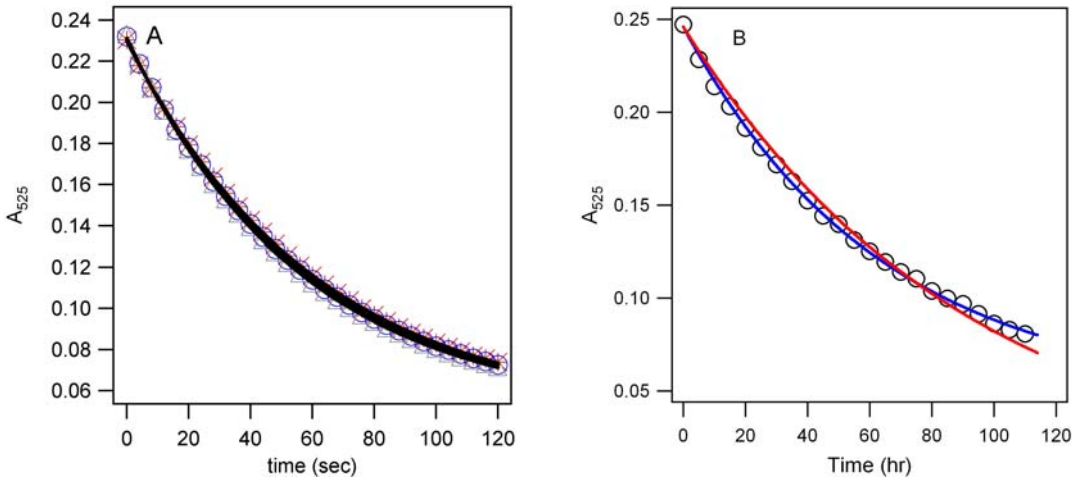

Figure 22: Data for the reactions of MnO_4^- with 3-chlorophenol and 1,4-dioxane (note the difference in time scales) with the fit to a simple first-order kinetic model (curve in red) and MnO_2-corrected model represented by equation 6 (curve in blue).

The k_{obs} values obtained by fitting equation 6 to experimental data were used to determine second-order rate constants, k''. For COCs with low solubility (< 0.002 M) or reaction rates (half-lives > 1.5 days), k'' was calculated with equation 7:

$$k'' = k_{obs} / [COC] \qquad [7]$$

For these COCs, the treatment effectively assumes the order of reaction with respect to the COC is one. The COCs for which k'' was determined this way were MTBE, toluene, PCE, picric acid, and 2,4-dinitrophenol. MTBE, PCE, and toluene have been shown by others to be first-order with respect to the COC (Gardner, 1996; Yan and Schwartz, 1999; Huang et al., 2001;

Damm et al., 2002). Picric acid and 2,4-dinitrophenol were assumed to be first-order with respect to COC based on their structural similarity to the mononitrophenols.

For COCs with sufficiently high solubilities that experiments could be set up over a significant range of initial COC concentrations ($[COC]_0$), we plotted k_{obs} vs. $[COC]_0$, determined that the plots were linear (and therefore approximately first order in [COC]), then fit the data by linear regression, and assigned the fitted slope to k''. Figures 3A and 3B illustrate this analysis for 3-chlorophenol and 1,4-dioxane, respectively.

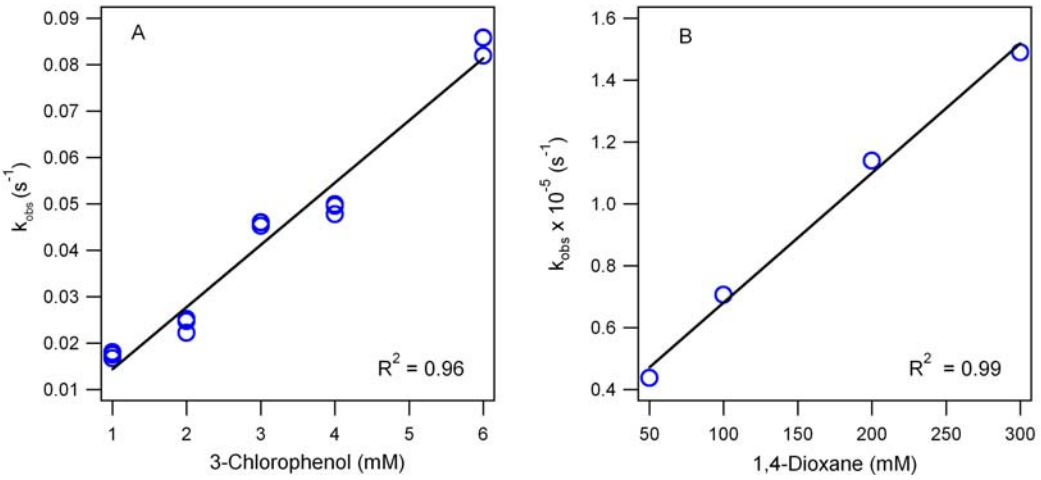

Figure 23: Data for the reactions of MnO_4^- with 3-chlorophenol and 1,4-dioxane: k_{obs} vs. concentration of COC plots; the slope of the regression line is used to determine k''.

In addition to absorption by MnO_2, another factor that can complicate the determination of k'' by measuring the disappearance of MnO_4^- rather than the COC is that MnO_4^- can be consumed by processes other than the primary reaction of interest: for example, the autodecomposition of MnO_4^- (even in pure water (Stewart, 1965)) and reaction with daughter products derived from the initial oxidation of the COC. Under the conditions used in this study, however, we found that autodecomposition of MnO_4^- was negligible. We also concluded that reaction of MnO_4^- with any daughter products of the COC oxidation was not likely to be significant because the COC concentration was high—at least 5-fold (and often >10-fold) greater than the MnO_4^-—and therefore would be the dominant reactant.

Further evidence that these (or other) factors did not significantly bias our measurement of k'' is provided by the strong correlation between values of k'' obtained from this study and previously published values of k'' that were obtained by analyzing decreasing concentrations of COC in the presence of excess MnO_4^- (Figure 4). In Figure 4, perfect agreement between our

data and literature data would fall on a line with slope = 1 and intercept = 0, which is shown for comparison.

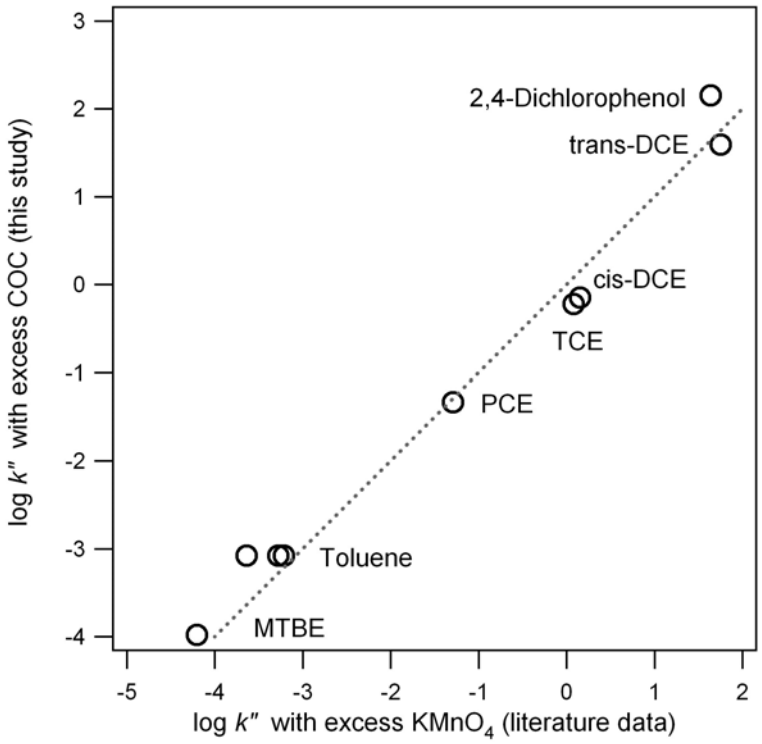

Figure 24: Correlation between *k″* obtained from pseudo-first-order conditions by either analyzing decreasing concentrations of MnO_4^- in the presence of an excess amount of COC (this study) or analyzing decreasing concentrations of COC in the presence of an excess amount of MnO_4^- (*k″* data obtained from the literature). Perfect agreement between the two sets of data would follow the dashed line. For the chlorinated ethenes, the literature values of *k″* used in this Figure are the values Huang et al. measured at 25 °C (Huang et al., 2001) because their experimental conditions most closely matched ours. Multiple literature values of *k″* for toluene are shown because the only literature value obtained at 25 °C was also obtained with excess COC conditions. For MTBE and 2,4-dichloro-phenol, no literature data from 25 °C were available for this comparison, so data for 23 and 16 °C, respectively, were used.

Figure 5 summarizes all values of *k″* that were measured in this study along with all values of *k″* that we found in the literature for MnO_4^- oxidation of potential COCs under relevant conditions. Inspection of the data in Figure 5 shows that variability in *k″* for any particular COC is generally less than 10-fold, while variability among closely related COCs is 2-3 orders of magnitude, and variability among families of unrelated COCs is almost 7 orders of magnitude. The variability in *k″* for any particular COC is satisfactory considering that the data often are from different laboratories obtained by different methods under slightly different conditions.

With respect to the variability in k'' within and across families of COCs, a general observation that can be made from Figure 5 is that a number of COCs react with MnO_4^- nearly as fast or faster than the chlorinated ethenes. This comparison is potentially significant because the chlorinated ethenes have been remediated successfully with MnO_4^- in field-scale applications of ISCO (Schnarr et al., 1998; Siegrist et al., 2001), and, therefore, it follows that the other fast-reacting COCs shown in Figure 5 (e.g., TNT, aldicarb, dichlorvos, many phenols, and some PAHs) are possible candidates for ISCO with MnO_4^-. Of course, having established that k'' is suitably large for these COCs, other factors—such as the effect of adsorption to soil or the potential to form toxic daughter products—need to be evaluated to establish treatability. Another useful generalization that can be made from Figure 5 concerns COCs that do not react rapidly with MnO_4^-. The families of COCs with values of k'' that are significantly below those of the chlorinated ethenes are the chlorinated methanes and ethanes, simple aromatics like benzene and toluene, most fuel oxygenates and solvent ethers, and some explosives (most notably RDX).

As part of this study, we have filled many of the priority data gaps that existed previously, including those for TNT, 1,4-dioxane, some pesticides, and many phenols. However, because our method requires that COCs have at least moderate solubility (~0.5 mM), we were not able to fill some data gaps for significant, low-solubility compounds—most notably pentachlorophenol, dibenzodioxins, polychlorinated biphenyls, and some of the more insoluble pesticides, such as 1,1,1-trichloro-2,2-bis(p-chlorophenyl)ethane (DDT), and dieldrin. Most of these COCs are included in Figure 5—even though no k'' data for them are available yet—so that the Figure provides a balanced perspective on current coverage of the whole range of potential COCs.

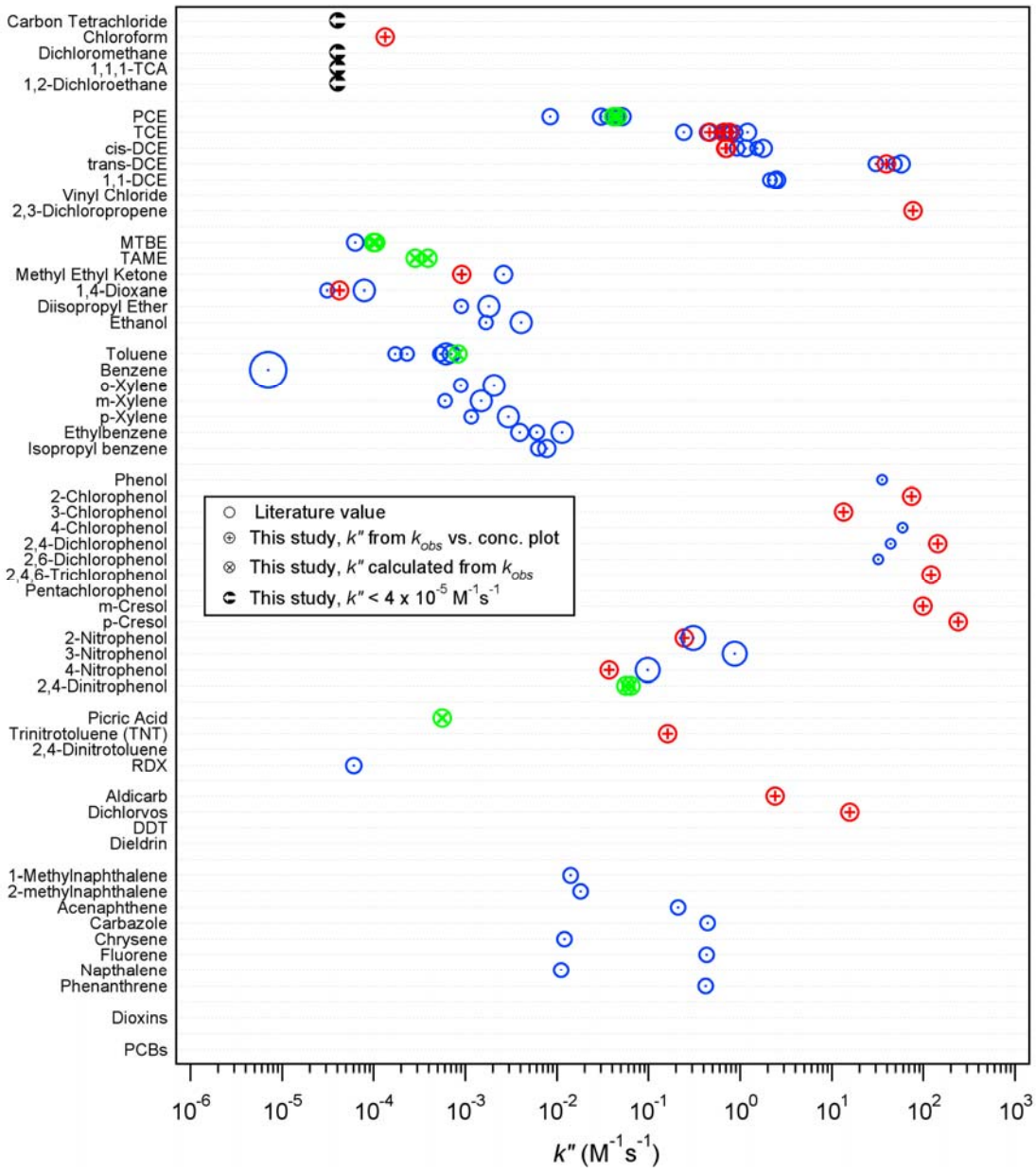

Figure 25: Summary of second-order rate constants (k'') for MnO_4^- and compounds in all classes. The size of the data points represent the temperature at which the data were collected; most of the temperatures for the literature values vary between 16 ºC to 35 ºC, the exception being that the k'' reported for benzene was determined at 70 ºC. The pH for the literature values of k'' ranges from 4.6 to 8.0. Compounds labeled in red text are too insoluble for the method we used. Experimental conditions for the data points from this study: 25 ºC, pH 7, and phosphate buffer concentrations between 50 - 100 mM.

7. Determining K" for Activated Hydrogen Peroxide[4]

An exhaustive literature review was performed to summarize existing kinetic data on the oxidation of NAPL constituents by activated hydrogen peroxide and hydroxyl radical. As expected, we found a large body of literature on the oxidation of contaminants by classical Fenton's reagent. However, in most cases, only first order kinetics are reported. In this literature, phenols are best represented with 24 papers (e.g., Chen and Pignatello, 1997; Esplugas et al., 2002) and oxygenates are least represented with only one paper (Burbano et al., 2002).

There is also a large body of literature reporting *k"* for contaminant degradation by •OH. However, in most cases the •OH is generated using non-Fenton's methods, such as gamma- or pulse-radiolysis (Farhataziz and Ross, 1977; Buxton et al., 1988), photo-Fenton's (Haag and Yao, 1992), and ozone plus hydrogen peroxide (Spanggord et al., 2000). In this literature, all chemical classes are well represented except pesticides. We identified only about ten papers that report *k"* of contaminant degradation by •OH generated by classic Fenton's reagent (Haag and Yao, 1992; Tang and Huang, 1996b; Tang and Huang, 1996a; Gallard et al., 1998; Benitez et al., 2000; Lindsey and Tarr, 2000; Watts et al., 2000; De Heredia et al., 2001; Gallard and De Laat, 2001). These ten papers include representatives of all chemical classes except explosives.

In our work on activated hydrogen peroxide, we set out to design experiments that would provide (first-order) kinetic data on key chlorinated solvents (priority contaminants for which *k"* are lacking) and a selective trap for hydroxyl radical (benzoic acid). We planned to use the latter data to normalize the former data, thereby extracting second-order rate constants (as illustrated in Figure 1).

Standard experimental conditions were choose were as follows: $[H_2O_2]$ = 8.8 mM, $[Fe^{2+}]$ = 0.45 mM (as $FeSO_4$), and $[Fe^{2+}]$:[H_2O_2] molar ratio = 1:19. All experiments used house-distilled water. Reaction mixtures were unbuffered and were adjusted to an initial pH of 3.0 using sulphuric acid. All Fenton experiments are being performed in a zero-headspace reactor, adapted from (Chen et al., 2001a; Chen et al., 2001b), which is shown in Figure 6.

[4] We have no publications planned from this part of the project.

Figure 26. Zero-headspace reactor used for to measure degradation kinetics by iron-activated hydrogen peroxide. Sampling is performed via the syringe.

Experiments were performed with a variety of chlorinated solvents—including trichloroethene (TCE) and 1,1-dichloroethene (DCE)—over a range of conditions. As an example, the conditions used for TCE are presented in Table 1.

Table 1. Initial conditions in the Fenton's System with TCE.

Exp	[TCE] (mg/l)	[H_2O_2] (mg/l)	[Fe^{2+}] (mg/l)	[TCE] (mmol/l)	[H_2O_2] (mmol/l)	[Fe^{2+}] (mmol/l)	TCE/H_2O_2/Fe^{2+} molar ratio
1-2	60	300	25	0.46	8.8	0.45	1:19:1
3-4	35	300	25	0.29	8.8	0.45	0.64:19:1
5-6	10	300	25	0.08	8.8	0.45	0.002:19:1

The results we obtained with each chlorinated solvent are illustrated in Figure 7 for TCE and DCE. Clearly, these data cannot be described by simple pseudo first-order disappearance kinetics. Using a more complex kinetic model that we developed, we were able to fit most aspects of these data (Figure 8).

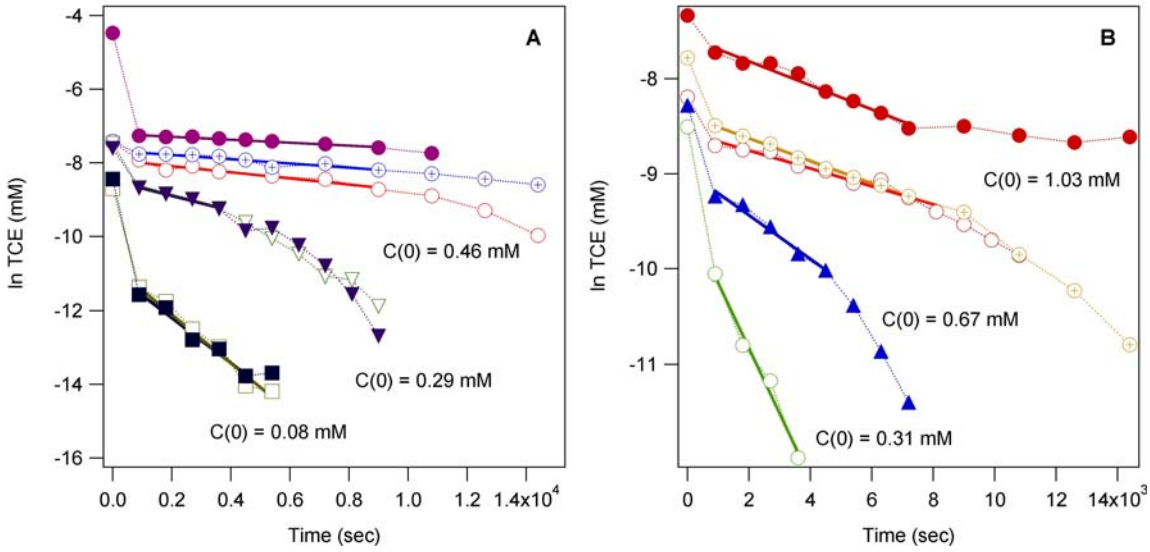

Figure 27. Disappearance kinetics for chlorinated solvents in a homogenous Fenton system: (A) TCE, and (B) 1,1-DCE. Solid lines illustrate fits to pseudo first-order kinetics.

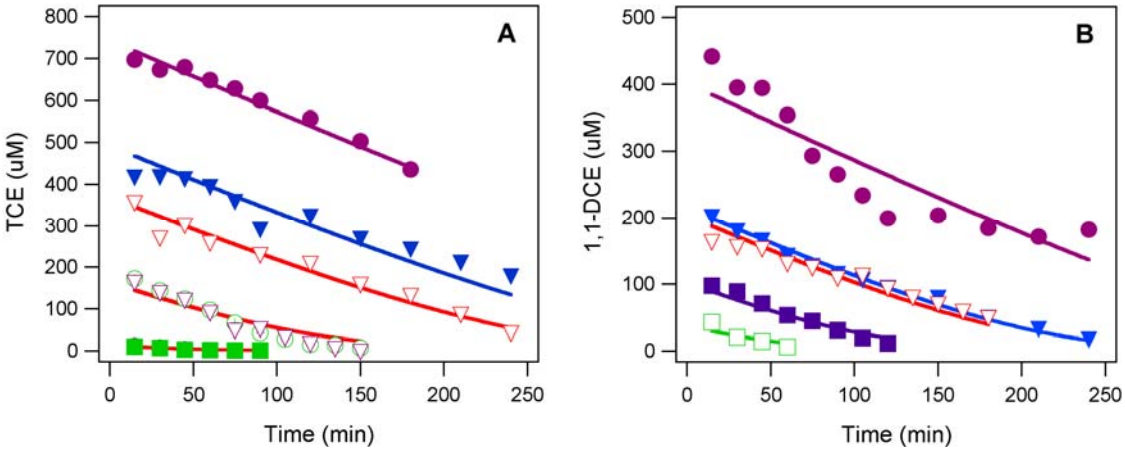

Figure 28. Modeling of kinetics for chlorinated solvents in a homogenous Fenton system: (A) TCE, and (B) 1,1-DCE. Solid lines are globally fit (across all sets of data in each plot) to a subset of the data.

Similarly complex kinetics were obtained with our hydroxyl radical trap benzoic acid (not shown). In an attempt to obtain a comprehensive interpretation and model for these data we collaborated with colleagues at the University of New South Wales who were just completing a multiyear effort to develop a fully-mechanistic model for the kinetics of Fenton system reactions (Duesterberg and Waite, 2006; Duesterberg and Waite, 2007). In principle, such a model could be used to extract high quality second-order rate constants for the reactions of •OH, test the

potential significance of other reactive oxygen species (e.g., superoxide), etc. Unfortunately, we were not able to get this model to fit all the key features of our data. We expect that there is some inconsistency in the data and/or the model, but it was beyond the resources of this project to resolve this. Instead, we turned out focus to activated persulfate, for which kinetic data for environmentally-relevant conditions are far more scarce.

8. Determining k" for Activated Persulfate[5]

Persulfate ($S_2O_8^{2-}$) was a more challenging oxidant to work with than permanganate and similar to H_2O_2 in that most of the observed oxidation of contaminants occurs via activation to •OH in the case of H_2O_2 and $SO_4^{\bullet-}$ in the case of $S_2O_8^{2-}$. The two general ways of activating $S_2O_8^{2-}$ are: homolysis of the peroxide bond using heat or light (equation 8) and an oxidation-reduction process (analogous to the Fenton reaction) with electron donors, including e^- (aq) from radiolysis of water or low-valent metals (Mn^+) such as Fe^{2+} and Ag^+ (equation 9).

$$S_2O_8^{2-} \xrightarrow{\text{heat or light}} 2SO_4^{\bullet-} \quad [8]$$

$$S_2O_8^{2-} + M^{n+} \longrightarrow M^{n+1} + SO_4^{\bullet-} + SO_4^{2-} \quad [9]$$

Once sulfate radical is generated, the following reactions have been speculated to occur:

$$SO_4^{\bullet-} + H_2O \rightleftharpoons HO^{\bullet} + H^+ + SO_4^{2-} \quad [10]$$

$$2\ SO_4^{\bullet-} \longrightarrow S_2O_8^{2-} \quad [11]$$

$$SO_4^{\bullet-} + HO^{\bullet} \longrightarrow HSO_5^- \quad [12]$$

$$2\ HO^{\bullet} \longrightarrow H_2O_2 \quad [13]$$

$$H_2O_2 \longrightarrow H_2O + 0.5\ O_2 \quad [14]$$

$$H_2O_2 + S_2O_8^{2-} \longrightarrow 2\ H^+ + 2SO_4^{2-} + O_2 \quad [15]$$

Determining *k″* for persulfate is complicated because it is the active species formed ($SO_4^{\bullet-}$)—not the persulfate itself—for which *k″* must be obtained. Often, to obtain *k″*, experiments are designed so that the reaction of the oxidant (Ox) with the COC is pseudo first-order. The second-order rate law can be written in two ways:

[5] Waldemer, R. H.; Tratnyek, P.G. (2007) Sulfate radical ($SO_4^{\bullet-}$) oxidation kinetics of organic contaminants in aquatic media. *Environ. Sci. Technol.,* in prep.

$$\frac{\partial[\mathrm{COC}]}{\partial \mathrm{t}} = k''[\mathrm{COC}][\mathrm{Ox}] \qquad [16]$$

$$\frac{\partial[\mathrm{Ox}]}{\partial \mathrm{t}} = k''[\mathrm{COC}][\mathrm{Ox}] \qquad [17]$$

Therefore, the experiment can be designed so either (*i*), the [COC] or (*ii*), the [Ox] is in significant excess (usually 10x the concentration of the other) and is effectively constant throughout the reaction; in other words, pseudo-first-order conditions.

However, a third option—the one employed here—is to use a competition kinetics method, in which *k″* is measured by d[probe]/dt, where the probe is a compound such as p-nitrosodimethylaniline (PNDA) that is easy to analyze (PNDA absorbs strongly at 440 nm) and is highly reactive with the oxidant (for example, *k″* for PNDA and $SO_4^{\bullet-}$ is 2.3 x 10^9 $M^{-1}s^{-1}$). The experimental set up for this method consists of several batch reactions with varying concentrations of COC and identical concentrations of PNDA and $SO_4^{\bullet-}$. In batch reactions with higher COC concentrations, the COC is better able to compete with the PNDA for available $SO_4^{\bullet-}$ (Fig 9A). The data can be linearized so *k″* can be determined (Fig 9B).

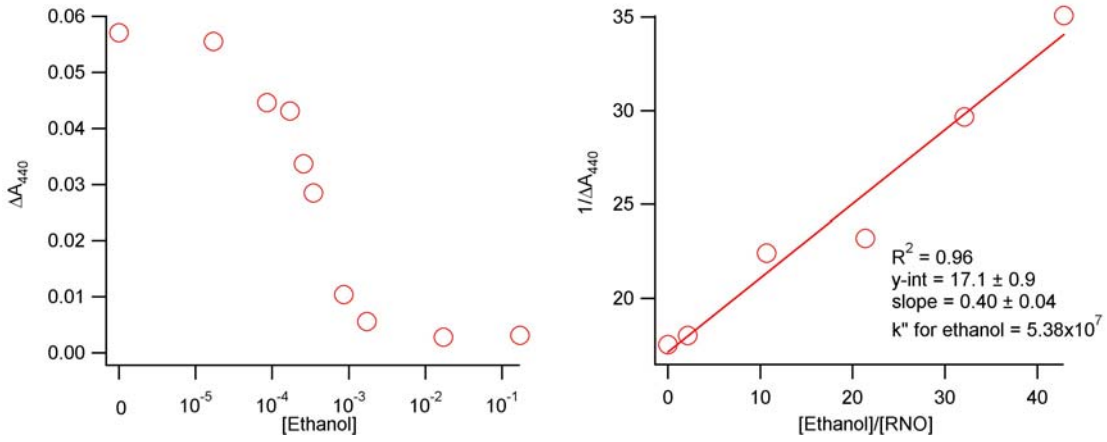

Figure 29: Typical competition kinetic plots. (A) Change in absorbance at 440 nm (indicating change in concentration of PNDA over 90 min); (B) Linear version of 1st six data points, used to calculate k″.

The main advantage of the competition kinetics method is that it allows *k″* for $SO_4^{\bullet-}$ to be determined without knowing the concentration of $SO_4^{\bullet-}$ in the reaction, which is difficult to do without the use of a stop-flow apparatus, often an expensive piece of equipment. The potential pitfalls of this method include the possibility that PNDA could react with the COC or its

daughter products in addition to the probe. In either case, simple competition kinetics will not apply, and the S-shaped curve typical of competition kinetics will not be obtained (Figure 10). A second problem would arise if the daughter products react with $S_2O_8^{2-}$ to produce additional $SO_4^{\bullet-}$; again, the S-shaped curve would not be obtained. In this case, at low COC concentrations, the PNDA is depleted more than it is when no COC is present due to the additional $SO_4^{\bullet-}$ in solution, but at high COC concentrations, the COC is able to effectively compete with PNDA despite the additional $SO_4^{\bullet-}$ in solution.

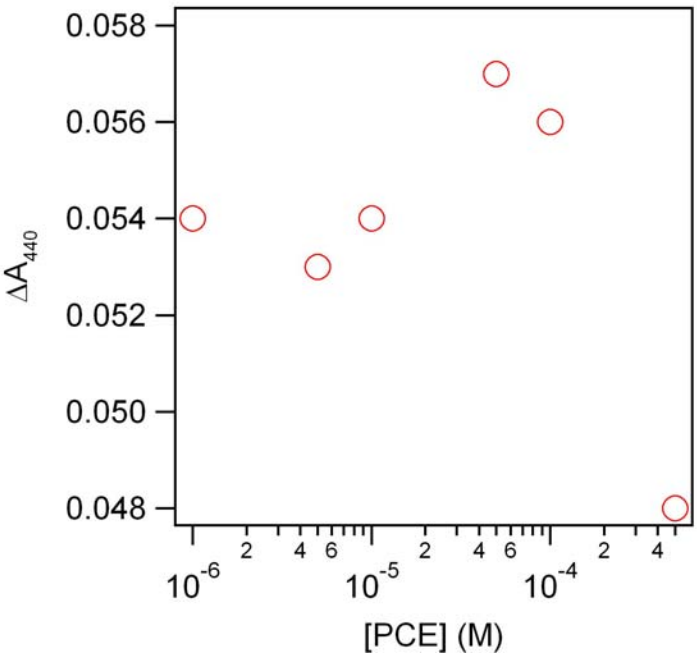

Figure 30: Data for perchloroethene (PCE) does not conform to the S-shaped curve typical of competition kinetics.

Although the competition method has several possible pitfalls, it must be remembered that issues arise with the more "traditional" methods of measuring k'' as well. In Section 6, we discussed possible problems with measuring d[Ox]/dt: namely, the possibility that the oxidant could react with daughter products or could be consumed by processes other than the primary reaction of interest (in the case of permanganate, this would be autodecomposition, while in the case of $SO_4^{\bullet-}$, this would be the reactions described by equations 10-12). In the case of persulfate, it is also possible for the daughter products to react with $S_2O_8^{2-}$ and produce additional $SO_4^{\bullet-}$, which would make the value of k'' artificially low. Similarly, when obtaining k'' by measuring d[COC]/dt, it is possible for the COC to react with species other than $SO_4^{\bullet-}$ that are generated from the activation of $S_2O_8^{2-}$ (see equations 10-15). Furthermore, for a study such as this one, where values of k'' for many COCs with very different chemical compositions are

desired, this approach is not practical, because a different analytical approach would have to be developed for each type of compound.

In light of all the possible issues with all methods of determining *k″*, it is important to validate the data by making comparisons among multiple methods (as we did for permanganate in Figure 4). The data from this study using competition kinetics is compared with data from the literature, which was obtained by measuring either d[$SO_4^{\bullet-}$]/dt or d[COC]/dt (Figure 11). The fact that the data (with the exception of MTBE) land on a one-to-one line is indicative that all methods, despite their potential pitfalls, are appropriate for measuring *k″*. Figure 11 also shows that in the experiments outlined for this study, the reactive species is $SO_4^{\bullet-}$, not •OH.

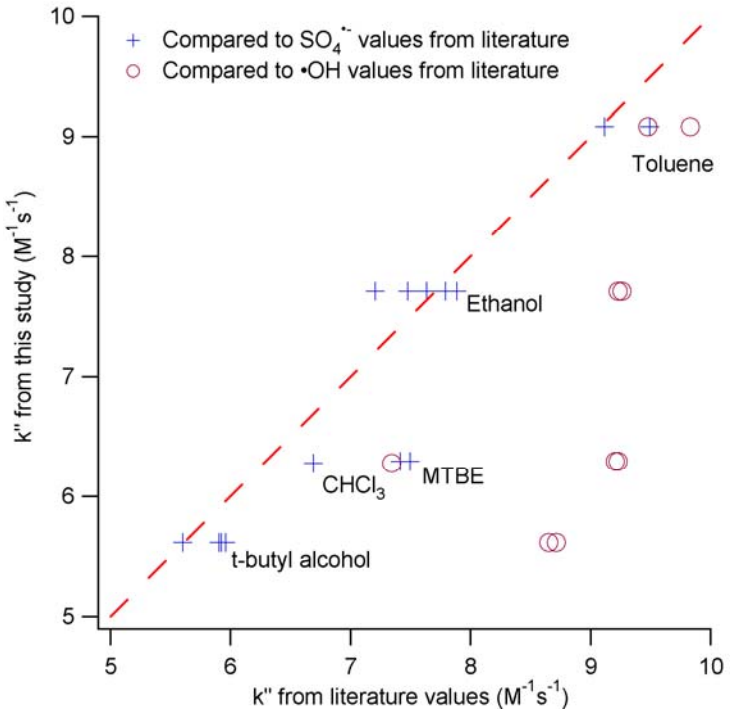

Figure 31: The values of *k″* obtained by this study with competition kinetics compared with values of *k″* for •OH and $SO_4^{\bullet-}$ obtained with either COC or $SO_4^{\bullet-}$ in excess (literature values).

The compilation of the data generated by competition experiments from this study and the rate constants obtained by the literature are shown in Figures 12 (aromatic compounds) and 13 (nonaromatic compounds). We have filled key data gaps for toluene, ethylbenzene, 2,4-dinitrotoluene, 2,6-dinitrotoluene, 1,1,1-trichloroethane, and 1,1,2-trichloroethane. Furthermore, we have added data for MTBE, t-butyl alcohol, chloroform, and ethanol. The chlorinated ethenes are a noticeable gap in the data; unfortunately, when the competition method was used

with these compounds, S-shaped curves were not obtained, indicating that *k″* could not be found using this probe.

When looking at Figures 12-13, one can see that for compounds with replicate data generated by multiple groups the agreement is almost always within half an order of magnitude. This is especially notable when considering this holds true even when $SO_4^{\bullet-}$ was generated in different ways (i.e. narrowband light, broadband light, heat, or iron). Thus, as expected, it appears that the method of persulfate activation does not greatly affect the value of *k″* for oxidation of COCs by $SO_4^{\bullet-}$.

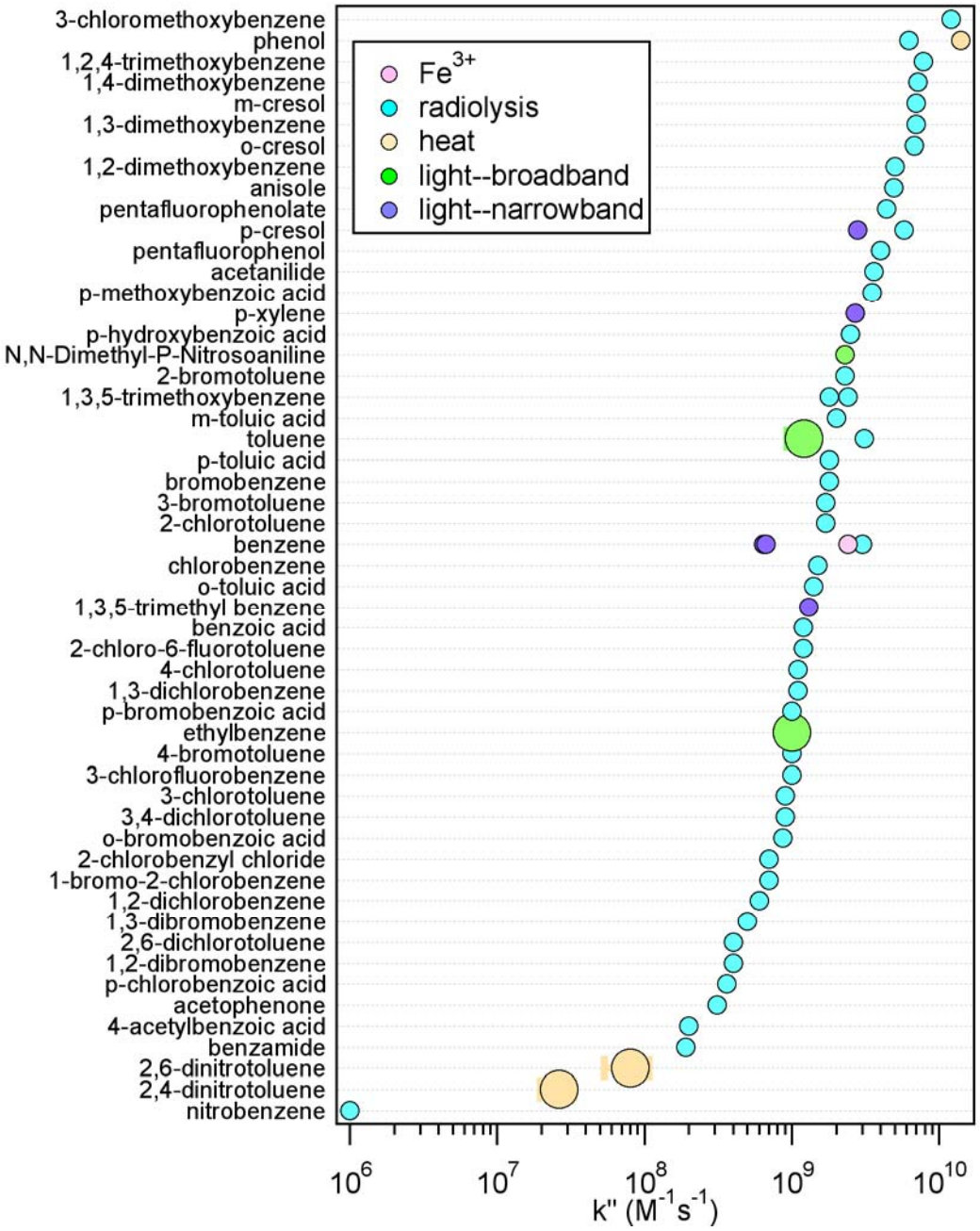

Figure 32. Summary of second-order rate constants (*k″*) for $SO_4^{\bullet-}$ and aromatic compounds. The big circles and error bars represent data obtained from this study, small circles represent literature values. The data are color coded by the method used to activate the persulfate.

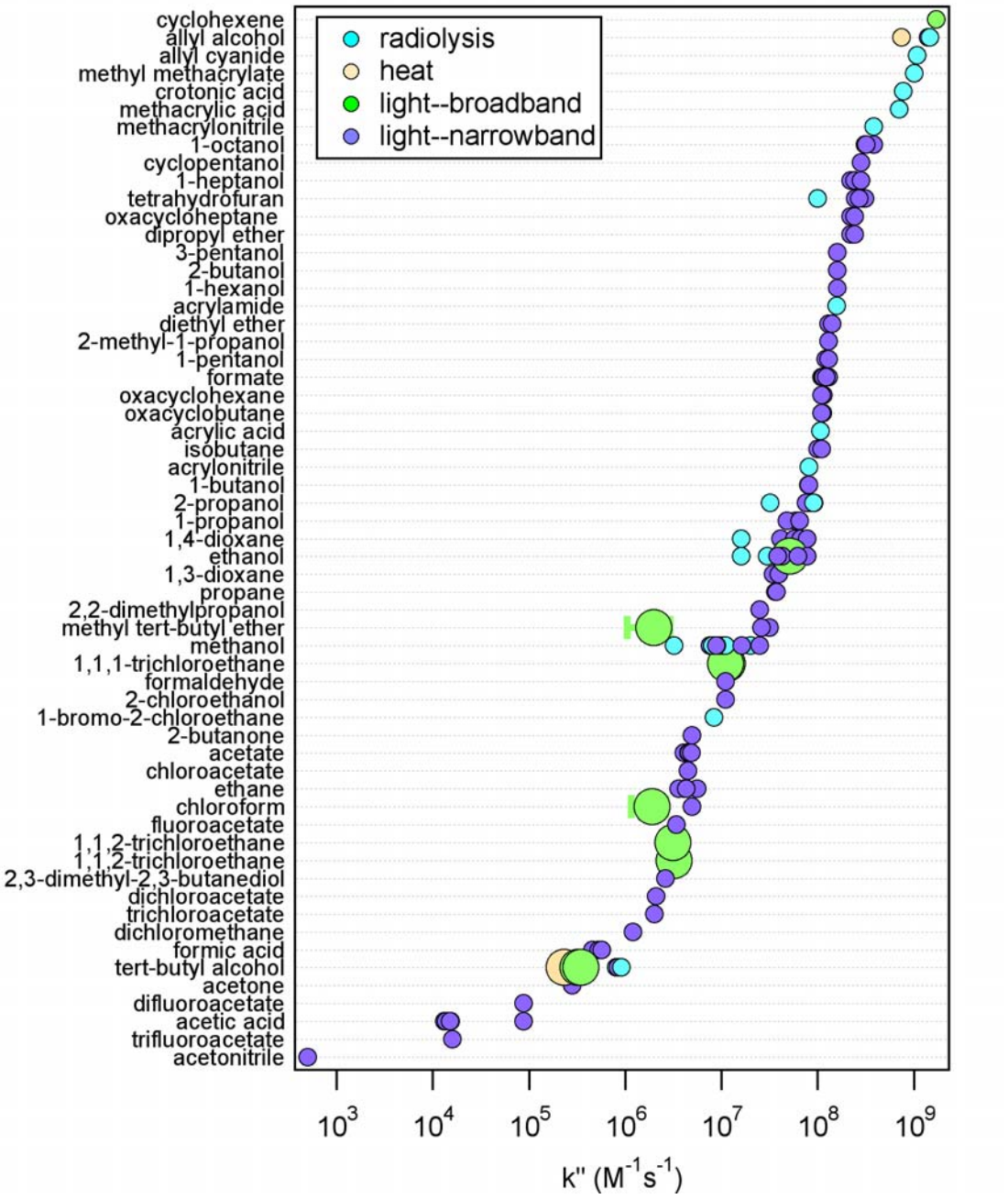

Figure 33. Summary of second-order rate constants (*k″*) for $SO_4^{\bullet-}$ and aliphatic compounds. The big circles and error bars represent data obtained from this study, small circles represent literature values. The data are color coded by the method used to activate the persulfate.

9. Correlation Analysis[6]

One of the goals of this study was to investigate whether quantitative structure-activity relationships (QSARs) could be developed for oxidations of COCs by MnO_4^-, $SO_4^{\bullet-}$, and •OH. The primary motivation for developing QSARs was to provide a means of predicting the rate of oxidation for compounds that have not been studied. A further benefit of developing QSARs is that evidence for a correlation (or lack of one) between chemical structure and reactivity with an oxidant can provide insight on the mechanism of oxidation with COCs. Because outliers often are easily identified when data are shown in this format, yet another benefit of QSARs is its usefulness in determining consistency among the data (Tratnyek, 1998).

In order to develop a successful QSAR among a group of compounds, the compounds must have similar reaction mechanisms or structurally similar reaction centers. In addition, a descriptor variable that relates to the reaction mechanism or reaction center must be identified. Descriptors that relate to the energetics of reaction include the half-wave potential ($E_{1/2}$), ionization potential (IP), and the energy of the highest occupied molecular orbital (E_{HOMO}). These may be preferred descriptors for oxidation reactions (Tratnyek, 1998; Canonica and Tratnyek Paul, 2003).

The descriptor that gave the best correlation for oxidation of COCs with $SO_4^{\bullet-}$ was E_{HOMO} (Figure 14), but the correlation is to complex to fit with a simple univariate QSAR model. Regretfully, we did not have the resources to explore more complex (nonlinear) models that might explain the data, we do not yet have a QSAR to report that can be used to predict values of *k″* for the oxidation reactions by $SO_4^{\bullet-}$ for COCs that have not been previously studied. However, the fact that the data set used for the correlation includes all the compounds shown in Figures 12 and 13, and the basic trend—that compounds with low values of E_{HOMO} are least reactive with $SO_4^{\bullet-}$—is upheld for the entire set, lends confidence that for most COCs, those with high values of E_{HOMO} will be most reactive with $SO_4^{\bullet-}$. Also shown in Figure 14 is that aromatic compounds tend to have the highest reactivity with $SO_4^{\bullet-}$, while nonaromatic compounds without double or triple bonds tend to have lower reactivity with $SO_4^{\bullet-}$. This observation gives insight into the mechanism of these oxidation reactions, implying that in addition to energetics, the electrophilic nature of $SO_4^{\bullet-}$ also plays a role in the oxidation of COCs.

---

[6] Waldemer, Rachel. H.; Kim, Jae-Hyoun; Tratynek, Paul G. (2007) Correlation analysis of kinetic data for aqueous oxidants. *Journal of Chemical Information and Modeling*; in prep.

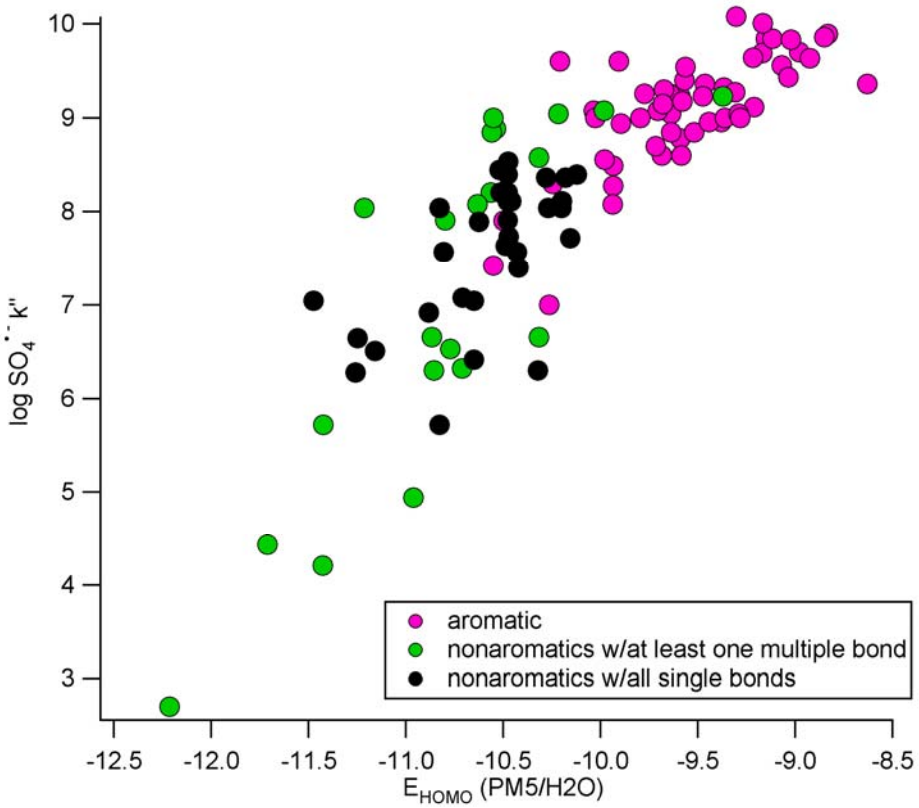

Figure 34. Correlation of *k″* for oxidation reactions of COCs by $SO_4^{\bullet-}$ to E_{HOMO}.

Unlike $SO_4^{\bullet-}$, oxidation by MnO_4^- of a large group of COCs containing different chemical subgroups is not described by a significant correlation to either E_{HOMO} or IP. Another descriptor that was explored is E_{GAP}: the energy difference between the HOMO and the lowest unoccupied molecular orbital (LUMO). E_{GAP} has been used as a measure of the relative stability of a compound toward chemical reaction—compounds with larger gaps are thought to have lower reactivity (Karelson, 2000; Miehr et al., 2004). However, the stability of the COC as measured by E_{Gap} also does not appear to predict the reactivity with MnO_4^-. Interestingly, the descriptor that seems to correlate best with reactivity of MnO_4^- among compounds of different chemical classes is the reactivity of these compounds with ozone (Figure 15). It is therefore likely that there are other effects in addition to electron transfer (perhaps steric effects) that are involved in the reaction of these compounds with MnO_4^-. If the unknown effects also affect the reactivity of compounds with ozone, these effects would be incorporated in the rate of oxidation by ozone.

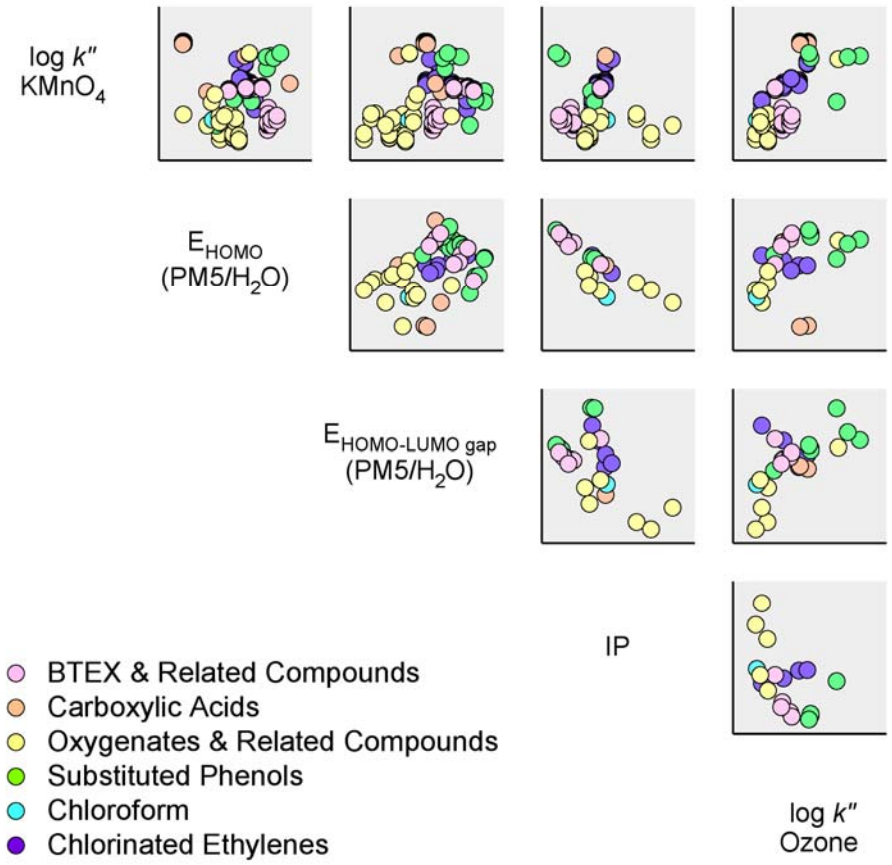

Figure 35. Scatter plot matrix of log *k″* of all compounds obtained from experiments or literature. All *k″* values were obtained at a pH between 4.0 and 8.0, at temperatures between 20°C and 30°C. E_{HOMO} and E_{Gap} were calculated with CAChe molecular modeling software. IP values were obtained from (Watanabe et al.; Kobayashi and Nagakura, 1974; Kobayashi and Nagakura, 1975). Ozone rate constants were obtained from (Hoigné and Bader, 1983b; Hoigné and Bader, 1983a; Hoigné et al., 1985).

Although a satisfactory correlation could not be found to describe oxidation by MnO_4^- for the entire dataset of COCs, a meaningful correlation was found for oxidation of the chlorinated ethenes (Figure 16). Because chlorine is an electron-withdrawing substituent, and the reactivity of the chlorinated ethenes decreases with increasing number of chlorines, MnO_4^- appears to be behaving as an electrophile in the initial rate-determining step, and it is likely that the electron density in the pi bonds of the chlorinated ethylenes, and not energetics, is controlling the reaction.

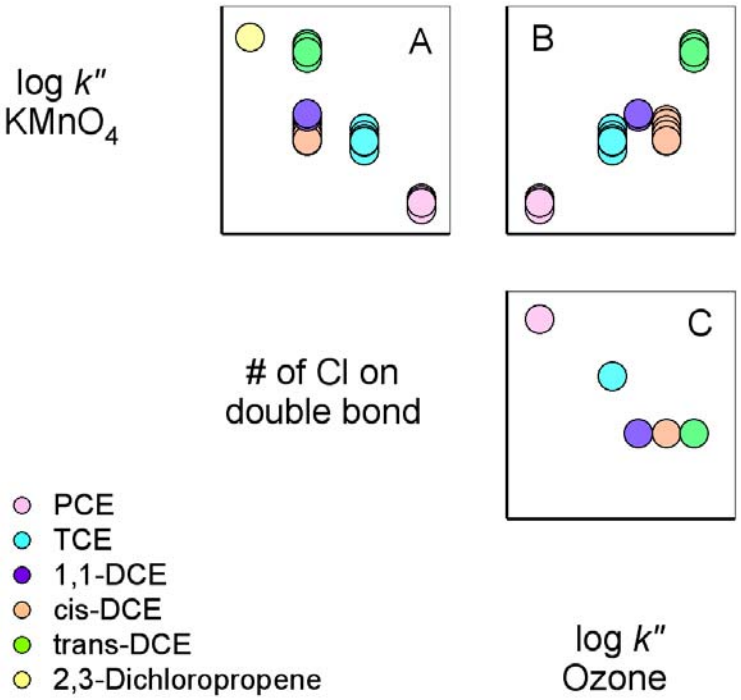

Figure 36. Matrix of scatter plots of log *k″* for MnO_4^- vs. the number of chlorine atoms attached to the double bond and vs. log *k″* for O_3. (Ozone data from (Hoigné and Bader, 1983a)).

In addition to the correlation of the rate constants for MnO_4^- and the chlorinated ethenes to the number of chlorine atoms on the double bond, there is also a satisfactory correlation with *k″* for the oxidation of these compounds by ozone. Direct ozonation of unsaturated compounds in low-pH aqueous media (the media used in the referenced ozone experiments) is generally agreed to occur through the formation of ozonide, another five-membered cyclic intermediate (Larson and Weber, 1994); therefore, it likely incorporates many of the rate-determining effects that are not described by the other descriptors. It is not surprising, then, that the rates of oxidation between ozone and MnO_4^- correlate so well—not only is there a high value of R^2 for the correlation (0.86), but it is clear that the correlation would be even better by removing the cis-DCE outlier. That the reaction rate of oxidation of cis-DCE by MnO_4^- is over-predicted by the rate of oxidation by ozone is likely because ozonide is less bulky than the cyclic hypomanganate diester formed by MnO_4^- oxidation, and is therefore not as greatly affected by steric hindrance from the close proximity of the chlorine atoms on cis-DCE.

Given that reactivity with ozone was the best descriptor for the entire dataset of kinetic data with MnO_4^-, upon gathering data for $SO_4^{\bullet-}$ and $^{\bullet}OH$ we included it in the cross-correlation

matrix. As can be seen in Figure 15, the only correlations with values of R^2 higher than 0.5 are between $SO_4^{\bullet-}$ and $^{\bullet}OH$, $SO_4^{\bullet-}$ and O_3, $^{\bullet}OH$ and O_3, and MnO_4^- and O_3. That $SO_4^{\bullet-}$ and $^{\bullet}OH$ correlate with each other but not MnO_4^- is likely indicative of the non-specific nature of the first two oxidants as compared to MnO_4^-. That all three of the aforementioned oxidants correlate to ozone may then seem surprising; however, this observation is easily explained by the fact that ozone can oxidize compounds directly, in the manner similar to MnO_4^- that was described earlier, or indirectly, through production of $^{\bullet}OH$ (Larson and Weber, 1994). It is likely that the compounds that correlate well with $SO_4^{\bullet-}$ and $^{\bullet}OH$ are oxidized by the indirect route, and the compounds that correlate well with MnO_4^- are oxidized directly. The oxidation of chloroform ($CHCl_3$) illustrates this point well. Chloroform is clearly an outlier in the correlations of $^{\bullet}OH$ and $SO_4^{\bullet-}$ with ozone, but not in the correlation of MnO_4^-, which may indicate that chloroform is oxidized by ozone directly.

10. IscoKin database[7]

In addition to our publications, we created a database containing our collection of k'' data that is available on the Internet at http://cgr.ebs.ogi.edu/iscokin. Access is unrestricted and we plan to keep the database online for the foreseeable future. A screen shot of the search interface is shown in Figure 17.

Unlike many online databases, which do not provide for automatic updating as new data become available, our database allows registered users to input new values of k''. This feature makes it possible for the ISCOKIN database to remain a current and complete resource for practitioners of ISCO and researchers interested in correlation analysis.

[7] http://cgr.ebs.ogi.edu/iscokin

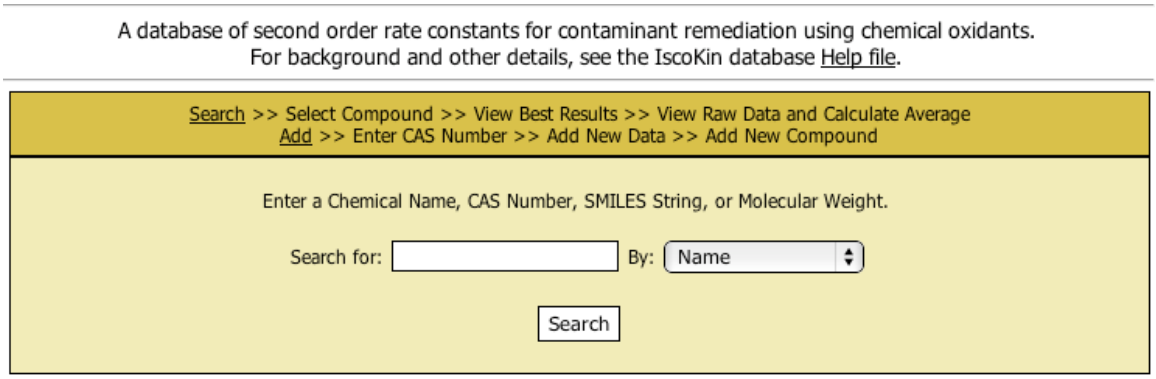

Figure 37. Screen shot of the initial search window for the IscoKin database. (http://cgr.ebs.ogi.edu/iscokin/search.php)

11. Oxidation of Chlorinated Ethenes by Heat-Activated Persulfate[8]

A potential advantage of $S_2O_8^{2-}$ is its stability before activation, which may allow delivery of the oxidant to contamination in hard to reach places. To take full advantage of this property, the best method of activating $S_2O_8^{2-}$ may be the remote, localized, and directed heating provided by some of the technologies used in ISTR. (For a review of ISTR heating technologies, see (Fountain, 1998).) This approach to activating $S_2O_8^{2-}$ contrasts favorably with activation methods that involve mixing reagents before injection (e.g., $S_2O_8^{2-}$ with chelated iron) because the latter inevitably result in reaction of some of the oxidant before it reaches the contaminated zone. In the case of $S_2O_8^{2-}$ activation with chelated iron, we expect that some of the $SO_4^{\bullet-}$ produced will react with excess Fe^{2+} ($k'' = 3–9.9 \times 10^8$ $M^{-1}s^{-1}$ (Heckel et al., 1966; McElroy and Waygood, 1990)) thereby lowering the concentration of $SO_4^{\bullet-}$ that is available to degrade contaminants. This effect may account for the observation that iron activation of $S_2O_8^{2-}$ is not always effective at degrading some contaminants that are degraded with $S_2O_8^{2-}$ activated by other methods (Block et al., 2004).

As mentioned earlier, once $S_2O_8^{2-}$ is activated (equations 8 or 9), the resulting $SO_4^{\bullet-}$ initiates a chain of reactions involving other radicals and oxidants (equations 10-15), some of which are potentially reactive intermediates, such as $^{\bullet}OH$ and peroxymonosulfate (HSO_5^-). The

[8] Waldemer, R. H.; Tratnyek, P.G.; Johnson, Richard L.; Nurmi, James T. (2007) Oxidation of chlorinated ethenes by heat activated persulfate: Kinetics and products. *Environ. Sci. Technol,.* 31(3), 1010-1015.

variety of intermediate oxidants generated in activated $S_2O_8^{2-}$ systems complicates the kinetics of contaminant oxidation. In principle, the contaminant disappearance should be describable with a pseudo-first-order rate constant that is the sum of second-order terms for each oxidant:

$$k_{obs} = k''_{SO_4^{\bullet-}}\left[SO_4^{\bullet-}\right] + k''_{HO^{\bullet}}\left[OH^{\bullet}\right] + k''_{S_2O_8^{2-}}\left[S_2O_8^{2-}\right] + k''_{other}\left[other\right] \qquad [18]$$

where k'' represents the second-order rate constants for the reaction of the contaminant with each reactive intermediate. Under most conditions, the dominant term in equation 18 is presumed to be the one involving $SO_4^{\bullet-}$ (Kolthoff et al., 1951; Peyton, 1993; Couttenye et al., 2002), which is why knowing k'' for the oxidation of $SO_4^{\bullet-}$ and COCs is valuable. However, it is not known how the relative significance of these terms varies with system parameters, such as temperature. Of course, k'' for all the terms in equation 18 will increase with temperature, resulting in faster oxidation of contaminants if the oxidant concentrations are not decreased. The latter, however, can not be assumed because the concentrations of $SO_4^{\bullet-}$ and other oxidants shown in equation 18 are the net result of many reactions (equations 8-15, the reactions of each oxidant with the contaminants and their byproducts, etc.), each of which will have its own dependence of rate on temperature. An additional uncertainty is the effect of temperature on the relative rates of contaminant degradation by chemical oxidants other than $S_2O_8^{2-}$ and background degradation processes such as hydrolysis. This study addresses these issues for the chlorinated ethenes by determining the temperature dependence of the kinetics and products of their oxidation by $S_2O_8^{2-}$, and comparing these results to calculations made from previously published data on the degradation of the chlorinated ethenes by permanganate and hydrolysis.

As shown in Figure 18 for PCE, oxidation of the chlorinated ethenes with thermally-activated $Na_2S_2O_8$ was pseudo-first-order for 1-2 half-lives at every temperature studied. In some cases, data were collected for more than two half-lives and the later time-points exhibited the distinctive downward curvature shown in Figure 19. The fact that this curvature can also be seen in previously published data for TCE and 1,1,1-trichloroethane oxidation by $S_2O_8^{2-}$ (Liang et al., 2003) suggests that the effect is not peculiar to the conditions of this study. The cause of this curvature was not explored in this or the previous studies, but it could be due to the combined reactivity of $SO_4^{\bullet-}$ and other reactive species that form as the reaction progresses, such as the organic radicals and chlorine radical ($Cl^{\bullet}$) that may be by-products of oxidation of chlorinated ethenes. To avoid having to model this phenomenon, we fit only the initial linear portion of the

data (1-2 half-lives) using the pseudo-first-order model. The resulting values of k_{obs} are given in Table 2 for the four chlorinated ethenes and five temperatures studied.

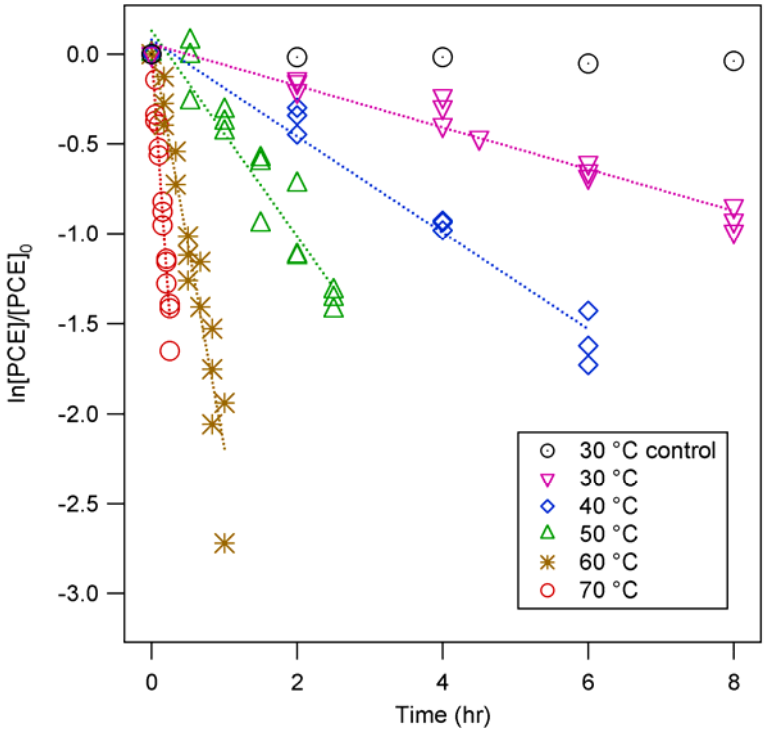

Figure 38. Pseudo-first-order disappearance of PCE at five temperatures. Experimental conditions: unbuffered, 4.5×10^{-5} M PCE, and 4.5×10^{-4} M $Na_2S_2O_8$. Triplicate experiments at each temperature. The control was done without persulfate.

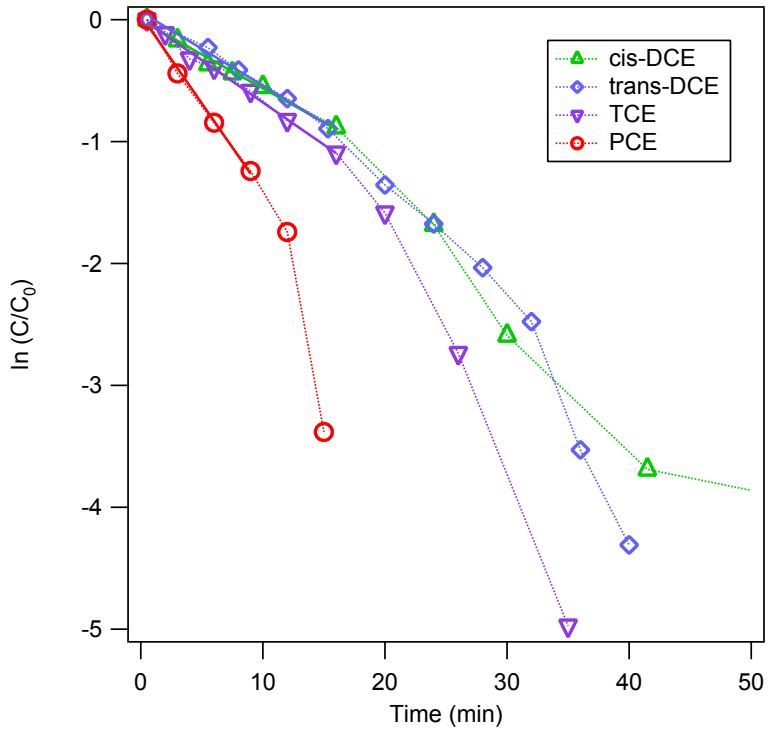

Figure 39. Concentration over extended time periods, showing non-pseudo first-order behavior at longer experimental times. Experimental conditions: Unbuffered DI water, 70 ^{o}C, 10:1 molar ratio of $Na_2S_2O_8$ and chlorinated ethenes, concentration of PCE = 0.0014 M, concentration of the other chlorinated ethenes = 0.002 M.

Table 2. k_{obs} and corresponding activation parameters for all 4 chlorinated ethenes

Compound	30°C		40 °C		50 °C		60 °C		70 °C		ln A (s^{-1})	E_A ($kJmol^{-1}$)
0.045 mM PCE	0.023 hr^{-1}	0.95	0.24 hr^{-1}	0.99	0.0087 min^{-1}	0.94	0.041 min^{-1}	0.98	0.11 min^{-1}	0.97	29 ± 2	101 ± 4
	0.027 hr^{-1}	0.97	0.25 hr^{-1}	0.96	0.0070 min^{-1}	0.91	0.030 min^{-1}	0.98	0.080 min^{-1}	0.99		
	0.031 hr^{-1}	0.97	0.24 hr^{-1}	0.96	0.0070 min^{-1}	0.97	0.034 min^{-1}	0.94	0.083 min^{-1}	0.97		
	0.060 hr^{-1}	0.99	----		----		----		----			
	0.055 hr^{-1}	0.99	----		----		----		----			
0.0014 M PCE	0.038 hr^{-1}	0.99	----		----		----		0.148 min^{-1}	0.99		
	0.040 hr^{-1}	0.99	----		----		----		0.145 min^{-1}	0.98		
	----		----		----		----		0.115 min^{-1}	0.98		
0.002 M TCE	0.027 hr^{-1}	0.98	0.073 hr^{-1}	0.94	0.0046 min^{-1}	0.96	0.0211 min^{-1}	0.99	0.061 min^{-1}	0.99	31 ± 1	108 ± 3
	0.031 hr^{-1}	0.97	0.087 hr^{-1}	0.97	0.0045 min^{-1}	0.97	0.0184 min^{-1}	0.99	0.067 min^{-1}	0.99		
	0.026 hr^{-1}	0.99	0.076 hr^{-1}	0.93	0.0051 min^{-1}	0.96	0.0179 min^{-1}	0.99	0.069 min^{-1}	0.9		
0.002 M cis-DCE	0.0033 hr^{-1}	0.93	0.023 hr^{-1}	0.96	0.0017 min^{-1}	0.94	0.008 min^{-1}	0.91	0.056 min^{-1}	0.99	43 ± 2	144 ± 5
	0.0034 hr^{-1}	0.96	0.022 hr^{-1}	0.99	0.0016 min^{-1}	0.98	0.0054 min^{-1}	0.99	0.068 min^{-1}	0.98		
	0.0032 hr^{-1}	0.95	0.026 hr^{-1}	0.99	----		0.005 min^{-1}	0.80	0.057 min^{-1}	0.99		
0.002 M trans-DCE	0.0048 hr^{-1}	0.97	0.033 hr^{-1}	0.99	0.0030 min^{-1}	0.98	0.018 min^{-1}	0.98	0.050 min^{-1}	0.99	43 ± 1	141 ± 2
	0.0060 hr^{-1}	0.96	0.038 hr^{-1}	0.99	0.0030 min^{-1}	0.99	0.017 min^{-1}	0.98	0.058 min^{-1}	0.99		
	0.0056 hr^{-1}	0.97	0.032 hr^{-1}	0.97	----		0.017 min^{-1}	0.97	0.059 min^{-1}	0.98		

For all four chlorinated ethenes, ln k_{obs} decreased linearly with 1/T (Figure 20) and, therefore, were fit to an Arrhenius-type model:

$$\ln k_{obs} = \ln A - E_A / RT \qquad [19]$$

where A is the pre-exponential factor, E_A is the apparent activation energy, R is the universal gas constant, and T is the absolute temperature. The fitting parameters from these calculations are presented in Table 3. Both ln A and E_A follow the pattern PCE < TCE < trans-DCE < cis-DCE; in fact, ln A and E_A correlate well with $R^2 = 0.99$ (Waldemer et al., 2007), a phenomenon that is fairly common but of uncertain significance (Philibert, 2006). A consequence of this is that k_{obs} also follows the pattern PCE > TCE > trans-DCE > cis-DCE and correlates with ln A and E_A (Waldemer et al., 2007). Additionally, ln A, E_A , and k_{obs} all correlate fairly well with the energy of the highest occupied molecular orbital (E_{HOMO}) for the chlorinated ethenes. This is to be expected because oxidation—regardless of the exact mechanism—generally involves a shift of electron density from the HOMO of the reductant (in this case, the chlorinated ethenes) to an electron acceptor (in this case, $SO_4^{\bullet -}$)(Canonica and Tratnyek, 2003).

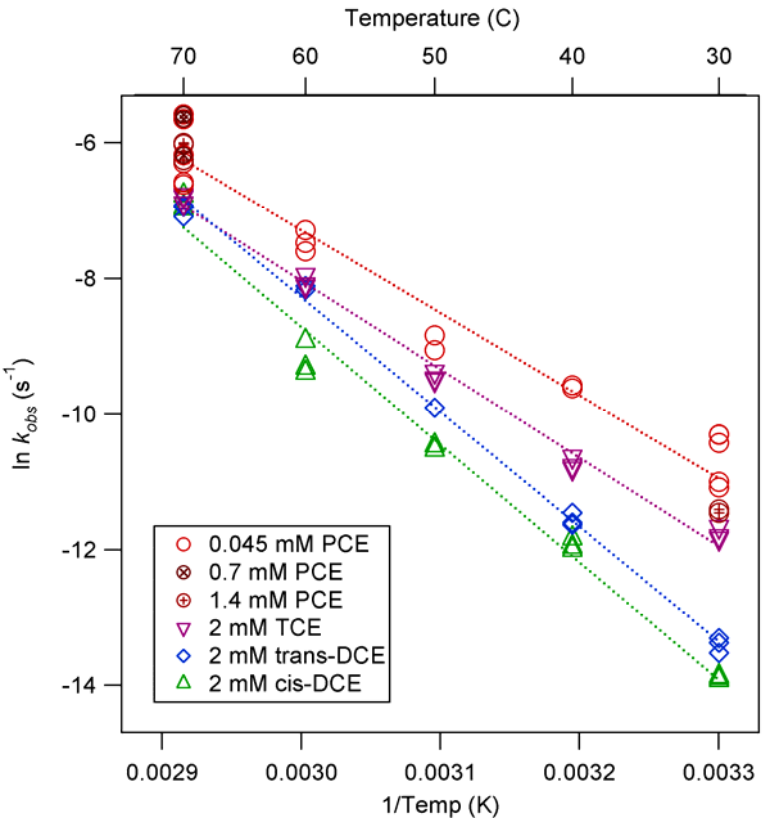

Figure 40 Arrhenius plots for the chlorinated ethenes. Experimental conditions: unbuffered, 10:1 molar ratio of $Na_2S_2O_8$ to chlorinated ethenes. Initial concentrations are given in the legend.

Table 3: Arrhenius parameters for chlorinated ethenes.

Compound	ln A (s^{-1})*	E_A (kJ/mol)*	N	R^2
PCE	29 ± 2	101 ± 4	25	0.96
TCE	31 ± 1	108 ± 3	15	0.99
cis-DCE	44 ± 2	144 ± 5	14	0.98
trans-DCE	43 ± 1	141 ± 2	14	0.99

*Uncertainties are one standard deviation derived from fitting equation 19 to the data in Figure 20.

Our value of E_A for TCE is within 10% of the value reported previously (97.7 kJ mol^{-1}) by Liang et al. (Liang et al., 2003). The only other data on E_A for oxidation of chlorinated ethenes by heat-activated $S_2O_8^{2-}$ are from Huang et al. (Huang et al., 2005). These values (PCE: 46.4, TCE: 60.7, cis-DCE: 41.4, trans-DCE: 49.8, 1,1-dichloroethene: 64.9, and vinyl chloride:

56.9 kJ mol^{-1}) are significantly lower (2-3 fold) than the values reported here (and by Liang et al. (Liang et al., 2003)), and the two sets of data do not correlate well (not shown). A likely explanation for this disagreement lies in the fact that Huang et al. measured degradation kinetics in a mixture of 59 contaminants (Huang et al., 2005). In such a situation, all of the contaminants—and possibly their degradation intermediates and products—can compete for $SO_4^{\bullet-}$ (and any other reactive species). If the various reactions have different activation energies, some contaminants will have proportionally higher reaction rates at the same temperature than others, and the contaminants with higher activation energies will become more effective competitors at higher temperatures. This competition effect could explain why the apparent activation energies for the chlorinated ethenes are lower in pseudo-first-order reactions with many other species present than when they are the only reductant in solution.

Little has been reported on the products of oxidation of the chlorinated ethenes by $S_2O_8^{2-}$, and there is no information on how the reaction pathways and products are affected by temperature. Anticipating some degree of mineralization, we measured Cl^- present at the end of experiments performed with the four chlorinated ethenes at 70 °C. For this purpose, we chose to run each experiment for a period anticipated to encompass 4 half-lives of contaminant degradation (~94%), which was estimated from the average of the pseudo-first-order rate constants listed in Table 2. Overall, Cl^- recoveries were consistent with complete dechlorination of 80-90% of each chlorinated ethene (data not shown). The only comparable literature data are for TCE, and they include Cl^- recoveries of 75% at 40°C, 80% at 50°C, and 85% at 60°C (Liang et al., 2003).

For systems containing $SO_4^{\bullet-}$, however, the interpretation of Cl^- data is complicated by the possibility that they react according to equation 20 ($k'' = 2.47 \times 10^8$ $M^{-1}s^{-1}$ (Huie and Clifton, 1990)). Then, the resulting chlorine radical, $Cl^{\bullet}$, can react with additional Cl^-, establishing an equilibrium with $Cl_2^{\bullet-}$ according to equation 21 ($k'' = 8 \times 10^9$ $M^{-1}s^{-1}$ (Huie and Clifton, 1990), K = 1.4×10^5 M^{-1} (Buxton et al., 2000)).

$$SO_4^{\bullet-} + Cl^- \longrightarrow Cl^{\bullet} + SO_4^{2-} \qquad [20]$$

$$Cl^{\bullet} + Cl^- \rightleftharpoons Cl_2^{\bullet-} \qquad [21]$$

Equation 21 suggests that the predominant chlorine radical species at the initiation of the Cl^- recovery experiments was $Cl^{\bullet}$, when the initial Cl^- concentration was very low (below detection),

and that $Cl_2^{\bullet-}$ should have become predominant by the end of each experiment (because degradation of the chlorinated ethenes produced final Cl^- concentrations 2-5 mM, which should shift equation 21 to favor $Cl_2^{\bullet-}$). One consequence of equations 20-21 could be depletion of Cl^-, but of greater interest is the possibility that $Cl^\bullet$ and $Cl_2^{\bullet-}$ react with the chlorinated ethenes or their intermediate degradation products to produce more highly chlorinated products, as has been reported previously for chlorinated phenols (Anipsitakis et al., 2006). The kinetic data necessary to evaluate how favorable chlorination of ethenes might be do not appear to be available, but we did detect trace quantities of hexachloroethane as intermediates in the oxidation of TCE and PCE.

The only chlorinated compounds that were identified as major intermediates were cis-DCE during trans-DCE oxidation and trans-DCE during cis-DCE oxidation. This evidence for racemization is shown in Figure 21 for 70 ^oC, but the effect was seen at all temperatures. Racemization presumably occurs after formation of a single-bonded intermediate, which might be the radical cation formed by electron-transfer to $SO_4^{\bullet-}$ (Minisci et al., 1983), or the $SO_4^{\bullet-}$-radical adduct, formed by asymmetric addition of $SO_4^{\bullet-}$ to the double bond. Evidence for the latter is strong, with many $SO_4^{\bullet-}$-radical adducts having been identified during reactions of $SO_4^{\bullet-}$ with alkenes by electron spin resonance (Chawla and Fessenden, 1975; Koltzenburg et al., 1982; Davies and Gilbert, 1984). It is less clear, however, what factors control the elimination of $SO_4^{\bullet-}$ to form the racemized DCE's.

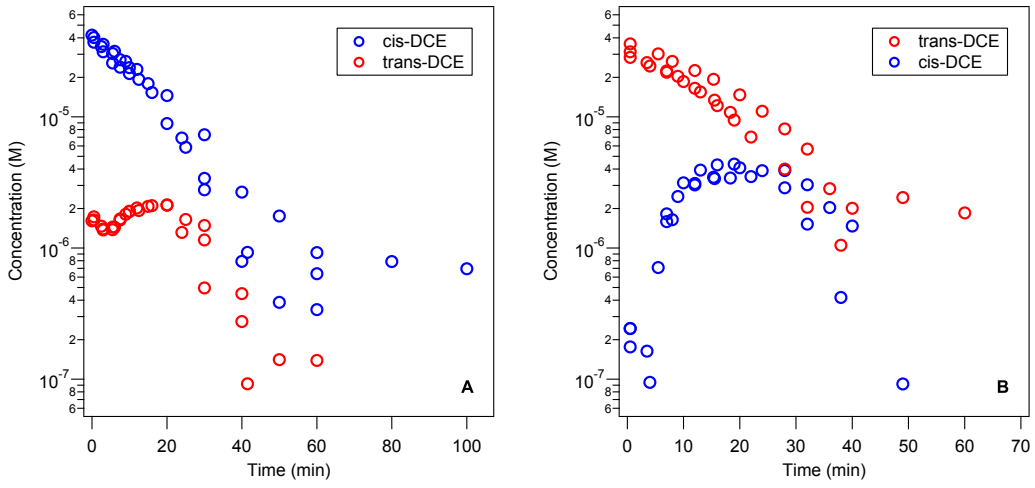

Figure 41. Concentration of cis-DCE and trans-DCE vs. time for A) the reaction of cis-DCE with persulfate and B) the reaction of trans-DCE with persulfate. Experimental conditions: unbuffered, triplicate experiments, 0.002 M dichloroethenes, 0.02 M $Na_2S_2O_8$, 70 ^oC.

To evaluate the potential benefits of coupling ISCO and ISTR for chlorinated ethenes, it is necessary to consider how temperature affects a variety of contaminant degradation processes. For hydrolysis and oxidation by permanganate, it is straightforward to calculate the respective values of k_{obs} vs. temperature (up to 100 ^{o}C) using equation 19 previously published Arrhenius parameters (Jeffers et al., 1989; Huang et al., 2001), and appropriate assumptions regarding the dose of permanganate (100-40,000 mg L^{-1}, 0.0007 M to 0.28 M (Siegrist et al., 2001)) and groundwater pH. For PCE, we show the results of these calculations in Figure 22, with the thickness of the bands reflecting the relevant ranges of permanganate concentration and pH. For the other chlorinated ethenes, we used only a representative permanganate concentration and pH, and the results are shown in Figure 23. Over the whole range of conditions considered, oxidation of the chlorinated ethenes is much faster than hydrolysis, although the opposite would have been the case for some of the more highly chlorinated ethanes. Additional factors must be considered for temperatures over 100 ^{o}C (Costanza et al., 2005).

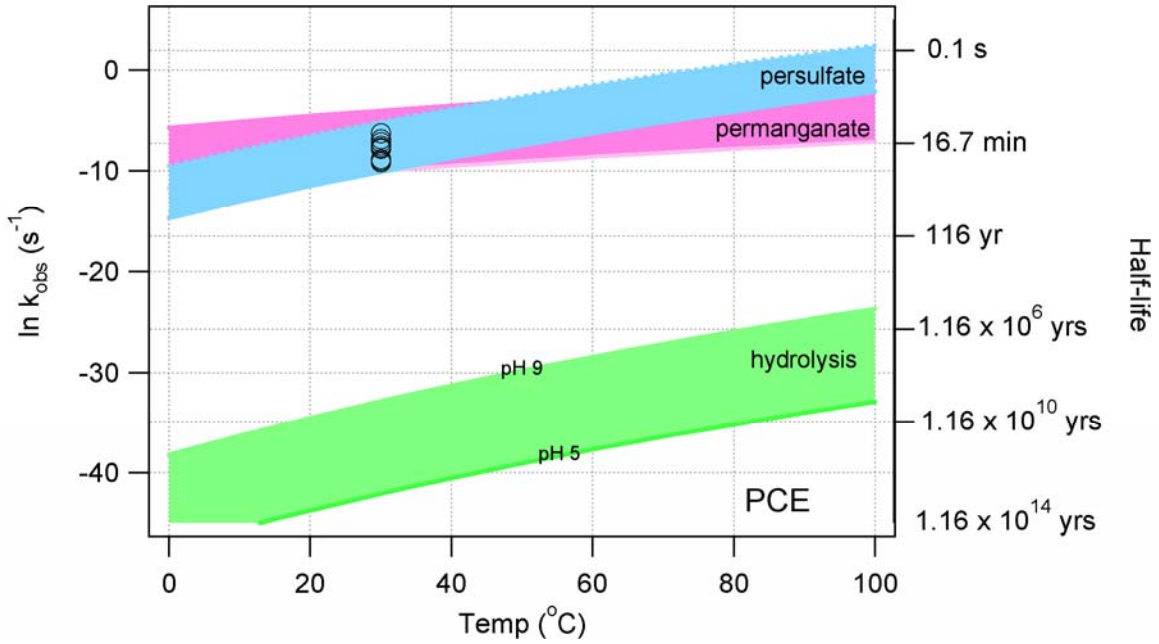

Figure 42. Comparison of three degradation processes for PCE as a function of temperature. The hydrolysis band was calculated using Arrhenius parameters obtained from (Jeffers et al., 1989). The bottom of the pink band corresponds to 100 mg/L (0.63 mM) permanganate and the to of this band corresponds to 40,000 mg/L (253 mM), calculated using Arrhenius parameters obtained from (Huang et al., 2001). The light blue band corresponds to Arrhenius parameters

obtained from experiments with 0.45 mM S_2O_8/0.045 mM PCE. The blue dots correspond to experimental data for varying concentrations of S_2O_8 while keeping the PCE concentration at 0.045 mM. The three concentrations represented by the three increasingly dark blue circles are: 4.5 mM S_2O_8, 45 mM S_2O_8, and 450 mM S_2O_8. The dashed blue line allows the reader to follow the likely Arrhenius progression of the 450 mM data at all temperatures.

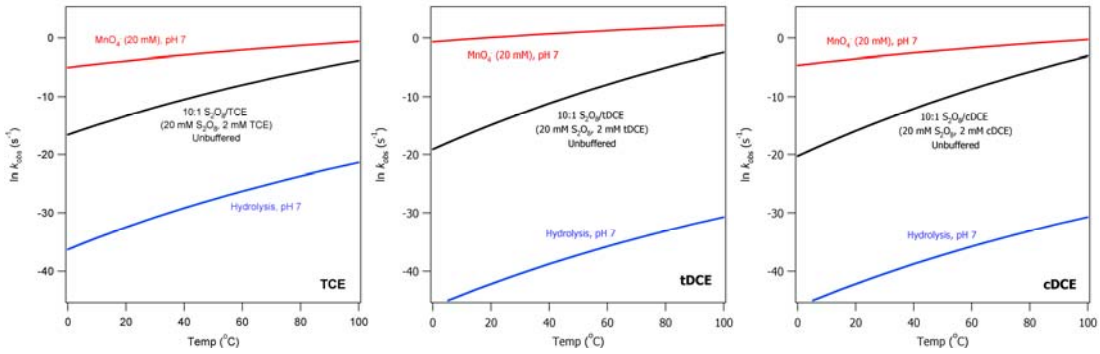

Figure 43. Comparison of three degradation processes as a function of temperature for TCE, cis-DCE, and trans-DCE. The hydrolysis band was calculated using Arrhenius parameters obtained from (Jeffers et al., 1989). The permanganate band was calculated using Arrhenius parameters obtained from (Huang et al., 2001). The persulfate band was calculated using Arrhenius parameters obtained from experiments with 20 mM $Na_2S_2O_8$ and 2 mM of the respective chlorinated ethenes

For contaminant oxidation by activated $S_2O_8^{2-}$, it is more difficult to develop a general description of k_{obs} vs. T because there are many reactions that can contribute to the concentration of the reactive intermediate $SO_4^{\bullet-}$ (equations 8-15, etc.), each with its own dependence on temperature. (Note that calculating the temperature dependence of contaminant oxidation by the Fenton reaction would pose a similar challenge.) To overcome this, we used the E_A for PCE that was determined in this study (Table 3) to fix the slope of the temperature dependence and estimated the intercept (ln A) from replicate experiments done at initial concentrations of $S_2O_8^{2-}$ ranging from 107 – 107,000 mg/L (0.00045 M to 0.45 M). This amounts to assuming that the apparent E_A is unaffected by $S_2O_8^{2-}$ concentration. The result, shown in Figure 22, reveals that the temperature at which the rate of PCE oxidation by heat-activated $S_2O_8^{2-}$ becomes greater than oxidation by permanganate is approximately 40 ^oC; and, by 100 ^oC, heat-activated $S_2O_8^{2-}$ oxidizes PCE about 400 times faster than permanganate. In contrast, the other chlorinated ethenes (Figure 23) are so much more reactive with permanganate that oxidation with activated

$S_2O_8^{2-}$ is slower even at 100 °C. The relative reactivity of PCE with these two oxidants is consistent with the relative reactivity of the chlorinated ethenes with each oxidant: PCE > TCE > cis-DCE > trans-DCE with activated $S_2O_8^{2-}$ (Figure 20) and the reverse with permanganate (Waldemer and Tratnyek, 2006).

While the comparisons facilitated by Figures 22 and 23 should be qualitatively accurate, the absolute rates we calculated may differ from those observed in the field for a variety of reasons. Prominent among the factors that suggest slower degradation rates under in situ conditions is the inefficiency of mixing of aqueous-phase oxidants with aqueous- and nonaqueous-phase contaminants because of aquifer heterogeneity (Seol et al., 2003), limited dispersion (especially vertical mixing (Johnson and Pankow, 1992)) and displacement of non-sorbing contaminants by the injected fluids. This limitation might be ameliorated by coupling ISCO with ISTR, because ISTR should encourage mixing of the oxidant plume with the contamination (by increasing flow within the heated zone due both to reduced water viscosity and increased buoyancy of the heated water). Another reason to expect slower oxidation rates in the field is that "natural oxidant demand" will suppress $SO_4^{\bullet-}$ concentrations (Brown and Robinson, 2004) leaving less $SO_4^{\bullet-}$ to oxidize contaminants. Here, again, coupling ISCO with ISTR may be advantageous, because $S_2O_8^{2-}$ will be relatively stable in unheated zones and heat-activation can be focused on contaminated zones. Additional factors remain to be investigated, such as thermal effects on geochemical processes that might, in turn, influence contaminant oxidation rates.

12. Effect of groundwater constituents on ISCO kinetics[9,10]

In general, we expect that k'' as defined throughout this project will depend on pH, temperature, and perhaps ionic strength, but not the concentrations of other groundwater constituents; whereas k_{obs} will also depend on the concentration of the oxidant and therefore be

---

[9] Waldemer, R. H.; Tratnyek, P.G.; Johnson, Richard L.; Nurmi, James T. (2007) Oxidation of chlorinated ethenes by heat activated persulfate: Kinetics and products. *Environ. Sci. Technol,.* 31(3), 1010-1015.

[10] Waldemer, R. H. (2004) Determination of the Rate of Contaminant Degradation by Permanganate: Implications for In Situ Chemical Oxidation (ISCO). M.S. thesis, OGI School of Science and Engineering, Portland, OR.

impacted by any processes that compete with the COC for the oxidant (Hoigné, 1990; Tratnyek and Macalady, 2000). The latter effect should be negligible for MnO_4^- because it reacts directly with COCs, and this is consistent with the observation that the rate of TCE oxidation by MnO_4^- is the same in "hard" tap water and in deionized water (Vella and Veronda, 1993). In contrast, activated persulfate and activated H_2O_2 react with COCs via reactive radicals that can be scavenged by dissolved carbonate and other species, which in turn makes k_{obs} for these treatment processes sensitive to the concentrations of such groundwater constituents (2005).

To verify that bicarbonate and other common groundwater constituents do not have a significant effect on rates of COC oxidation by MnO_4^-, we measured k_{obs} for oxidation of TCE over a range of concentrations for the major groundwater constituents. Bicarbonate concentrations in the range of 50 to 400 mg/L often occur in groundwater, with concentrations above 1000 mg/L possible; nitrate concentrations in groundwater are mostly below 20 mg/L, but groundwater contaminated with fertilizers can have concentrations above 1000 mg/L; and sulfate concentrations in groundwater tend to range from under 15 mg/L to about 500 mg/L (Matthess, 1982). Therefore, we chose to study the effect of 0 to 1000 mg/L nitrate (0–15.9 mM), sulfate (0–10.4 mM), and bicarbonate (0–16.4 mM) on the oxidation of TCE (1.0 mM) by MnO_4^- (0.1 mM). As expected, the rates (k_{obs} and k'') were not affected by any of the above groundwater constituents over the range of concentration studied (data shown in (Waldemer, 2004)).

As mentioned earlier, unlike oxidation reactions with MnO_4^-, we did expect environmental concentrations of carbonate species to affect k_{obs} for oxidation by activated $S_2O_8^{2-}$. To determine the degree of this effect on heat-activated $S_2O_8^{2-}$, PCE was used as the model compound along with 100, 300, and 500 mg L^{-1} of bicarbonate at 30, 50, and 70 ^oC. The data were fit to pseudo first-order kinetics—as shown in Figure 22 for 30 ^oC—and the resulting values of k_{obs} are given in Table 4. At all temperatures, bicarbonate inhibited the oxidation of PCE by activated $S_2O_8^{2-}$ (Figure 23). The inhibitory effect of bicarbonate appears to be steeper than a simple exponential relationship and equivalent at all three temperatures, but we did not attempt to model this behavior.

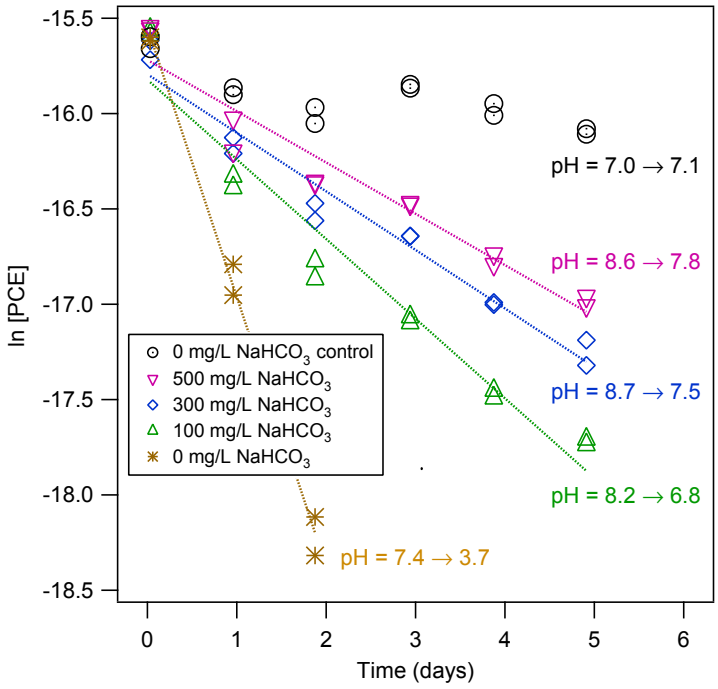

Figure 44. Effect of bicarbonate on the oxidation of PCE by persulfate. Experimental conditions: 30 °C, 4.5×10^{-5} M PCE, 4.5×10^{-4} M $Na_2S_2O_8$, two replicates. The control did not contain persulfate or bicarbonate.

The inhibitory effect of bicarbonate probably reflects competition between the PCE and bicarbonate for $SO_4^{\bullet-}$, but changes in pH could also be contributing. For all the experiments shown in Figure 23, the final pH decreased—possibly due to the release of protons when $SO_4^{\bullet-}$ reacts with water (equation 10)—and the degree of pH decrease was less pronounced with increased bicarbonate concentration (Figure 22). However, even with bicarbonate present, the oxidation of PCE still follows the Arrhenius model (shown in (Waldemer et al., 2007)) and the activation energies are not statistically different with bicarbonate or without it (Table 3).

Table 4: k_{obs} and corresponding activation parameters for PCE with different concentrations of bicarbonate

Bicarbonate (mg L^{-1})	30°C	50°C	70°C	ln A (s^{-1})	E_A (kJ mol^{-1})
0	See Table 1	See Table 1	See Table 1	29 ± 2	101 ± 4
100	0.018	0.30	0.84	25 ± 2	94 ± 5
300	0.013	0.12	1.62	26 ± 5	97 ± 12
500	0.011	0.15	1.32	26 ± 1	96 ± 2

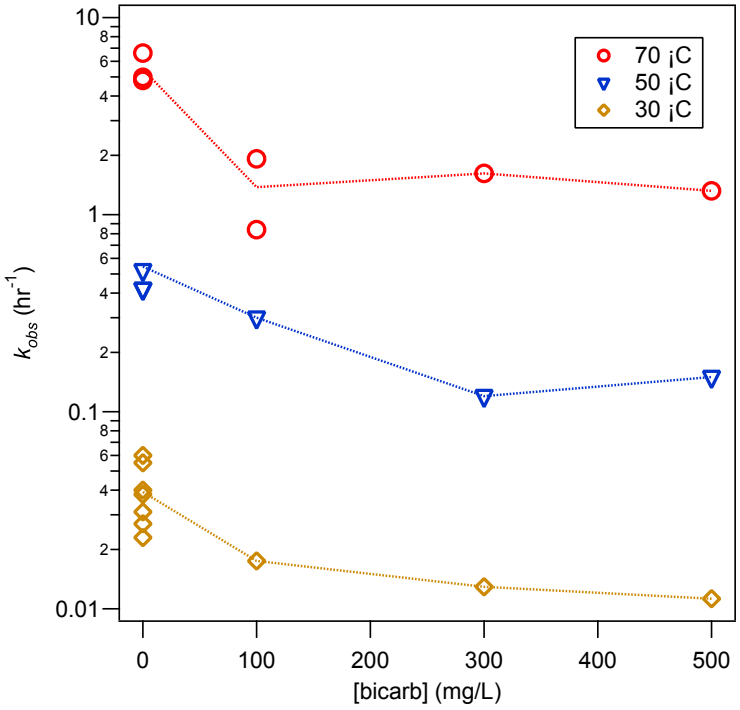

Figure 45. Effect of bicarbonate concentration on k_{obs} for PCE oxidation by persulfate activated at three temperatures. 4.5 × 10^{-5} M PCE, 4.5 × 10^{-4} M $Na_2S_2O_8$.

13. References

1. 2005. Interstate Technology and Regulatory Council (ITRC), pp. 172.
2. Anipsitakis, G.P., Dionysiou, D.D., Gonzalez, M.A., 2006. Cobalt-mediated activation of peroxymonosulfate and sulfate radical attack on phenolic compounds. Implications of chloride ions. *Environ. Sci. Technol.,* **40,** 1000-1007.
3. Augusti, R., Kias, A.O., Rocha, L.L., Lago, R.M., 1998. Kinetics and mechanism of benzene derivative degradation with Fenton's reagent in aqueous medium studied by MIMS. *J. Phys. Chem. A,* **102,** 10723-19727.
4. Benitez, F.J., Beltran-Heredia, J., Acero, J.L., Rubio, F.J., 2000. Contribution of free radicals to chlorophenols decomposition by several advanced oxidation processes. *Chemosphere,* **41,** 1271-1277.
5. Bier, E.L., Singh, J., Li, Z.M., Comfort, S.D., Shea, P.J., 1999. Remediating hexahydro-1,3,5-trinitro-1,2,5-trazine-contaminated water and soil by fenton oxidation. *Environ. Toxicol. Chem.,* **18,** 1078-1084.
6. Block, P.A., Brown, R.A., Robinson, D., 2004. In *Proceedings of the Fourth International Conference on Remediation of Chlorinated and Recalcitrant Compounds, 24-27 May 2004, Monterey, CA*(Ed., Gavaskar, A.R.C., A. S. C.) Battelle Press, Columbus, OH, pp. 2A-05.
7. Brown, R.A., Robinson, D., 2004. Response to naturally occurring organic material: permanganate versus persulfate. In *Proceedings of the Fourth International Conference on Remediation of Chlorinated and Recalcitrant Compounds, 24-27 May 2004, Monterey, CA*Battelle Press, Columbus, OH, pp. 2A.06/01-02A.06/08.
8. Burbano, A.A., Dionysiou, D.D., Richardson, T.L., Suidan, M.T., 2002. Degradation of MTBE intermediates using Fenton's reagent. *J. Environ. Eng.,* **128,** 799-805.
9. Buxton, G.V., Bydder, M., Salmon, G.A., Williams, J.E., 2000. The reactivity of chlorine atoms in aqueous solution. Part III. The reactions of Cl· with solutes. *Phys. Chem. Chem. Phys.,* **2,** 237-245.
10. Buxton, G.V., Greenstock, C.L., Helman, W.P., Ross, A.B., 1988. Critical review of rate constants for reactions of hydrated electrons, hydrogen atoms and hydroxyl radicals (•OH/•O-) in aqueous solution. *J. Phys. Chem. Ref. Data,* **17,** 513-886.
11. Canonica, S., Tratnyek Paul, G., 2003. Quantitative structure-activity relationships for oxidation reactions of organic chemicals in water. *Environ. Toxicol. Chem.,* **22,** 1743-1754.
12. Canonica, S., Tratnyek, P.G., 2003. Quantitative structure-activity relationships (QSARs) for oxidation reactions of organic chemicals in water. *Environ. Toxicol. Chem.,* **22,** 1743-1754.
13. Chawla, O.P., Fessenden, R.W., 1975. Electron spin resonance and pulse radiolysis studies of some reactions of SO_4^-. *J. Phys. Chem.,* **79,** 2693-2700.
14. Chen, G., Hoag, G.E., Chedda, P., Nadim, F., Woody, B.A., Dobbs, G.M., 2001a. The mechanism and applicability of in situ oxidation of trichloroethylene with Fenton's reagent. *J. Hazard. Mater.,* **87,** 171-186.

15. Chen, J.L., Al-Abed, S.R., Ryan, J.A., Li, Z., 2001b. Effects of pH on dechlorination of trichloroethylene by zero-valent iron. *J. Hazard. Mater.,* **83,** 243-254.

16. Chen, R., Pignatello, J.J., 1997. Role of quinone intermediates as electron shuttles in Fenton and photoassisted Fenton oxidations of aromatic compounds. *Environ. Sci. Technol.,* **31,** 2399-2406.

17. Costanza, J., Davis Eva, L., Mulholland James, A., Pennell Kurt, D., 2005. Abiotic degradation of trichloroethylene under thermal remediation conditions. *Environ. Sci. Technol.,* **39,** 6825-6830.

18. Couttenye, R.A., Huang, K.-C., Hoag, G.E., Suib, S.L., 2002. Evidence of sulfate free radical ($SO4^{-\cdot}$) formation under heat-assisted persulfate oxidation of MTBE. *Proceedings of the Petroleum Hydrocarbons and Organic Chemicals in Ground Water: Prevention, Assessment, and Remediation, Conference and Exposition, 19th, Atlanta, GA, USA, Nov. 5-8, 2002,* 345-350.

19. Damm, J.H., Hardacre, C., Kalin, R.M., Walsh, K.P., 2002. Kinetics of the oxidation of methyl tert-butyl ether (MTBE) by potassium permanganate. *Water Research,* **36,** 3638-3646.

20. Davies, M.J., Gilbert, B.C., 1984. Electron spin resonance studies. Part 68. Addition versus overall one-electron abstraction in the oxidation of alkenes and dienes by $SO_4^{-\cdot}$, $Cl_2^{-\cdot}$, and $^{\cdot}OH$ in acidic aqueous solution. *J. Chem. Soc., Perkin Trans. 2,* 1809-1815.

21. De Heredia, J.B., Torregrosa, J., Dominguez, J.R., Peres, J.A., 2001. Kinetic model for phenolic compound oxidation by Fenton's reagent. *Chemosphere,* **45,** 85-90.

22. Duesterberg, C.K., Waite, T.D., 2006. Process optimization of fenton oxidation using kinetic modeling. *Environ. Sci. Technol.,* **40,** 4189-4195.

23. Duesterberg, C.K., Waite, T.D., 2007. Kinetic modeling of the oxidation of p-hydroxybenzoic acid by Fenton's reagent: Implications of the role of quinones in the redox cycling of iron. *Environ. Sci. Technol.,* **41,** 4103-4110.

24. Esplugas, S., Gimenez, J., Contreras, S., Pascual, E., Rodriguez, M., 2002. Comparison of different advanced oxidation processes for phenol degradation. *Water Research,* **36,** 1034-1042.

25. Farhataziz, Ross, A.B., 1977. *Selected Specific Rates of Reactions of Transients from Water in Aqueous Solution III. Hydroxyl Radical and Perhydroxyl Radical and Their Radical Ions,* U. S. Department of Commerce, Washington D.C.

26. Farrell, J., Luo, J., 2002. Grand canonical Monte Carlo study of sediment-contaminant interactions. *Preprints of Extended Abstracts presented at the ACS National Meeting, American Chemical Society, Division of Environmental Chemistry,* **42,** 123-126.

27. Fountain, J.C., 1998. Ground-Water Remediation Technologies Analysis Center, Pittsburgh.

28. Gallard, H., De Laat, J., 2001. Kinetics of oxidation of chlorobenzenes and phenyl-ureas by Fe(II)/H2O2 and Fe(III)/H2O2. Evidence of reduction and oxidation reactions of intermediates by Fe(II) or Fe(III). *Chemosphere,* **42,** 405-413.

29. Gallard, H., de Laat, J., Legube, B., 1998. Effect of pH on the oxidation rate of organic compounds by Fe-II/H2O2. Mechanisms and simulation. *New J. Chem.,* **22,** 263-268.

30. Gardner, K.A., 1996. In *Chemistry*University of Washington, Seattle, WA, pp. 133.

31. Gardner, K.A., Mayer, J.M., 1995. Understanding C-H bond oxidations: H• and H– transfer in the oxidation of toluene by permanganate. *Science,* **269,** 1849-1851.

32. Geosyntec Consultants, Oregon Health and Science University, and University of Waterloo, 2003. An Improved Understanding of In Situ Chemical Oxidation (CU-1289): FY03Annual Report. 29 November, 2003.

33. Geosyntec Consultants, Oregon Health and Science University, and University of Waterloo, 2005. An Improved Understanding of In Situ Chemical Oxidation (CU-1289): FY04 Annual Report. 5 January, 2005.

34. Goldstein, S., Meyerstein, D., 1999. Commentary: Comments on the mechanism of the "Fenton-like" reaction. *Acc. Chem. Res.,* **32,** 547-550.

35. Haag, W.R., Yao, C.C.D., 1992. Rate constants for reaction of hydroxyl radicals with several drinking water contaminants. *Environ. Sci. Technol.,* **26,** 1005-1013.

36. Heckel, E., Henglein, A., Beck, G., 1966. Pulse radiolytic investigation of the radical anion $SO_4^{\cdot-}$. *Ber. Bunsen-Ges.,* **70,** 149-154.

37. Hoigné, J., 1990. Formulation and calibration of environmental reaction kinetics: Oxidations by aqueous photooxidants as an example. In *Aquatic Chemical Kinetics: Reaction Rates of Processes in Natural Waters*Wiley-Interscience, New York, pp. 43-70.

38. Hoigné, J., Bader, H., 1983a. Rate constants of reactions of ozone with organic and inorganic compounds in water—I. Non-dissociating organic compounds. *Water Research,* **17,** 173-183.

39. Hoigné, J., Bader, H., 1983b. Rate constants of reactions of ozone with organic and inorganic compounds in water—II. Dissociating organic compounds. *Water Research,* **17,** 185-194.

40. Hoigné, J., Bader, H., 1993. Kinetics of reactions involving chlorine dioxide (OClO) in water—I. Inorganic and organic compounds. *Water Research,* **28,** 45-55.

41. Hoigné, J., Bader, H., Haag, W.R., Staehelin, J., 1985. Rate constants of reactions of ozone with organic and inorganic compounds in water—III: Inorganic compounds and radicals. *Water Research,* **19,** 993-1004.

42. Hong, A., Zappi, M.E., Kuo, C.H., Hill, D., 1996. Modeling kinetics of illuminated and dark advanced oxidation processes. *J. Environ. Eng.,* **122,** 58-62.

43. Hood, E.D., Thomson, N.R., Grossi, D., Farquhar, G.J., 2000. Experimental determination of the kinetic rate law for the oxidation of perchloroethylene by potassium permanganate. *Chemosphere,* **40,** 1383-1388.

44. Huang, K.C., Hoag, G.E., Chheda, P., Woody, B.A., Dobbs, G.M., 1999. Kinetic study of oxidation of trichloroethylene by potassium permanganate. *Environ. Eng. Sci.,* **16,** 265-274.

45. Huang, K.C., Hoag, G.E., Chheda, P., Woody, B.A., Dobbs, G.M., 2001. Oxidation of chlorinated ethenes by potassium permanganate: A kinetics study. *J. Hazard. Mater.,* **87,** 155-169.

46. Huang, K.C., Zhao, Z.Q., Hoag, G.E., Dahmani, A., Block, P.A., 2005. Degradation of volatile organic compounds with thermally activated persulfate oxidation. *Chemosphere,* **61,** 551-560.

47. Huie, R.E., Clifton, C.L., 1990. Temperature dependence of the rate constants for reactions of the sulfate radical, SO_4^-, with anions. *J. Phys. Chem.,* **94,** 8561-8567.

48. Huston, P.L., Pignatello, J.J., 1996. Reduction of perchloroalkanes by ferrioxalate-generated carboxylate radical preceding mineralization by the photo- fenton reaction. *Environ. Sci. Technol.,* **30,** 3457-3463.

49. Jeffers, P.M., Ward, L.M., Woytowitch, L.M., Wolfe, N.L., 1989. Homogeneous hydrolysis rate constants for selected chlorinated methanes, ethanes, ethenes, and propanes. *Environ. Sci. Technol.,* **23,** 965-969.

50. Johnson, R.L., Pankow, J.F., 1992. Dissolution of dense chlorinated solvents into groundwater. 2. Source functions for pools of solvent. *Environ. Sci. Technol.,* **26,** 896-901.

51. Karelson, M., 2000. *Molecular descriptors in QSAR/QSPR,* John Wiley & Sons, Inc., New York.

52. Kobayashi, T., Nagakura, S., 1974. Photoelectron spectra of substituted benzenes. *Bull. Chem. Soc. Jpn.,* **47,** 2563-2572.

53. Kobayashi, T., Nagakura, S., 1975. Photoelectron spectra of nitrophenols and nitroanisoles. *J. Electron Spectrosc. Relat. Phenom.,* **6,** 421-427.

54. Kolthoff, I.M., Medalia, A.I., Raaen, H.P., 1951. The reaction between ferrous iron and peroxides. IV. Reaction with potassium persulfate. *J. Am. Chem. Soc.,* **73,** 1733-1739.

55. Koltzenburg, G., Behrens, G., Schulte-Frohlinde, D., 1982. Fast hydrolysis of alkyl radicals with leaving groups in the beta position. *J. Am. Chem. Soc.,* **104,** 7311-7312.

56. Larson, R.A., Weber, E.J., 1994. Chapter 4. Environmental Oxidations. In *Reaction Mechanisms in Environmental Organic Chemistry*Lewis, Chelsea, MI, pp. 217-273.

57. Leung, S.W., Watts, R.J., Miller, G.C., 1992. Degradation of perchloroethylene by Fenton's reagent: speciation and pathway. *J. Environ. Qual.,* **21,** 377-381.

58. Li, Z.M., Comfort, S.D., Shea, P.J., 1997. Destruction of 2,4,6-trinitrotoluene by fenton oxidation. *Journal of Environmental Quality,* **26,** 480-487.

59. Liang, C.J., Bruell, C.J., Marley, M.C., Sperry, K.L., 2003. Thermally activated persulfate oxidation of trichloroethylene (TCE) and 1,1,1-trichloroethane (TCA) in aqueous systems and soil slurries. *Soil Sed. Contam.,* **12,** 207-228.

60. Lindsey, M.E., Tarr, M.A., 2000. Quantitation of hydroxyl radical during Fenton oxidation following a single addition of iron and peroxide. *Chemosphere,* **41,** 409-417.

61. Lipczynska-Kochany, E., 1991. Degradation of aqueous nitrophenols and nitrobenzene by means of the Fenton reactions. *Chemosphere,* **22,** 529-536.

62. MacFaul, P.A., Wayner, D.D.M., Ingold, K.U., 1998. Commentary: A Radical Account of "Oxygenated Fenton Chemistry". *Acc. Chem. Res.,* **31,** 159.

63. Mata-Perez, F., Perez-Benito, J.F., 1985. Identification of the product from the reduction of permanganate ion by trimethylamine in aqueous phosphate buffers. *Can. J. Chem.,* **63,** 988-992.

64. Matthess, G., 1982. *The Properties of Groundwater,* Wiley, New York.

65. Mayer, J.M.M., 1998. Hydrogen atom abstraction by metal-oxo complexes: Understanding the analogy with organic radical reactions. *Acc. Chem. Res.,* **31,** 441-450.

66. McElroy, W.J., Waygood, S.J., 1990. Kinetics of the reactions of the SO_4^- radical with SO_4^-, $S_2O_8^{2-}$, H_2O, and Fe^{2+}. *J. Chem. Soc., Faraday Trans.,* **86,** 2557-2564.

67. Miehr, R., Tratnyek, P.G., Bandstra, J.Z., Scherer, M.M., Alowitz, M., Bylaska, E.J., 2004. The diversity of contaminant reduction reactions by zero-valent iron: role of the reductate. *Environ. Sci. Technol.,* **38,** 139-147.

68. Minisci, F., Citterio, A., Giordano, C., 1983. Electron-transfer processes: peroxysulfate, a useful and versatile reagent in organic chemistry. *Acc. Chem. Res.,* **16,** 27-32.

69. Perez-Benito, J.F., Arias, C., 1992. Occurrence of colloidal manganese dioxide in permanganate reactions. *J. Colloid Interface Sci.,* **152,** 70-84.

70. Peyton, G.R., 1993. The free-radical chemistry of persulfate-based total organic carbon analyzers. *Mar. Chem.,* **41,** 91-103.

71. Philibert, J., 2006. Some thoughts and/or questions about activation energy and pre-exponential factor. *Defect and Diffusion Forum,* **249,** 61-72.

72. Pignatello, J.J., Oliveros, E., MacKay, A., 2006. Advanced oxidation processes for organic contaminant destruction based on the Fenton reaction and related chemistry. *Crit. Rev. Environ. Sci. Technol.,* **36,** 1-84.

73. Sawyer, D.T., Sobkowiak, A., Matsushita, T., 1996. Metal [ML(x); M=Fe, Cu, Co, Mn]/hydroperoxide-induced activation of dioxygen for the oxygenation of hydrocarbons: oxygenated Fenton chemistry. *Acc. Chem. Res.,* **29,** 409-416.

74. Schnarr, M., Truax, C., Farquhar, G., Hood, E., Gonullu, T., Stickney, B., 1998. Laboratory and controlled field experiments using potassium permanganate to remediate trichloroethylene and perchloroethylene DNAPLs in porous media. *J. Contam. Hydrol.,* **29,** 205-224.

75. Sedlak, D.L., Andren, A.W., 1991. Oxidation of chlorobenzene with Fentons' Reagent. *Environ. Sci. Technol.,* **25,** 777-782.

76. Seol, Y., Zhang, H., Schwartz, F.W., 2003. A review of in situ chemical oxidation and heterogeity. *Environ. Eng. Geosci.,* **9,** 37-49.

77. Siegrist, R.L., Urynowicz, M.A., West, O.A., Crimi, M.L., Lowe, K.S., 2001. *Principles and Practices of In Situ Chemical Oxidation Using Permanganate,* Battelle Press, Columbus, OH.

78. Spanggord, R.J., Yao, C.D., Mill, T., 2000. Oxidation of aminodinitrotoluenes with ozone: Products and pathways. *Environ. Sci. Technol.,* **34,** 497-504.

79. Stewart, R., 1965. Oxidation by permanganate. In *Oxidation in Organic Chemistry*, Vol. 5A Academic Press, New York, pp. 1-68.

80. Tang, W.Z., Huang, C.P., 1996a. 2,4-dichlorophenol oxidation kinetics by Fenton's reagent. *Environmental Technology,* **17,** 1371-1378.

81. Tang, W.Z., Huang, C.P., 1996b. An oxidation kinetic model of unsaturated chlorinated aliphatic compounds by Fenton's reagent. *Journal of Environmental Science and Health, Part A- Environmental Science and Engineering & Toxic and Hazardous Substance Control,* **31,** 2755-2775.

82. Tang, W.Z., Tassos, S., 1997. Oxidation kinetics and mechanisms of trihalomethanes by Fenton's reagent. *Water Research,* **31,** 1117-1125.

83. Tratnyek, P.G., 1998. Correlation analysis of the environmental reactivity of organic substances. In *Perspectives in Environmental Chemistry*Oxford, New York, pp. 167-194.

84. Tratnyek, P.G., Hoigné, J., 1991. Oxidation of substituted phenols in the environment: a QSAR analysis of rate constants for reaction with singlet oxygen. *Environ. Sci. Technol.,* **25,** 1596-1604.

85. Tratnyek, P.G., Macalady, D.L., 2000. Oxidation-reduction reactions in the aquatic environment. In *Handbook of Property Estimation Methods for Chemicals: Environmental and Health Sciences*Lewis, Boca Raton, FL, pp. 383-415.

86. Vella, P.A., Veronda, B., 1993. Oxidation of trichloroethylene: A comparison of potassium permanganate and Fenton's reagent. *Chemical Oxidation,* **3,** 62-73.

87. Waldemer, R.H., 2004. OGI School of Science and Engineering, Oregon Health and Science UniversityEditor, Portland, OR, pp. 86.

88. Waldemer, R.H., Tratnyek, P.G., 2004. The efficient determination of rate constants for oxidations by permanganate. In *Proceedings of the Fourth International Conference on Remediation of Chlorinated and Recalcitrant Compounds, 24-27 May 2004, Monterey, CA*Battelle Press, Columbus, OH, pp. Paper 2A-09.

89. Waldemer, R.H., Tratnyek, P.G., 2006. Kinetics of contaminant degradation by permanganate. *Environ. Sci. Technol.,* **40,** 1055-1061.

90. Waldemer, R.H., Tratnyek, P.G., Johnson, R.L., Nurmi, J.T., 2007. Oxidation of chlorinated ethenes by heat activated persulfate: Kinetics and products. *Environ. Sci. Technol.,* **31,** 1010-1015.

91. Walling, C., 1998. Commentary: Intermediates in the reactions of Fenton type reagents. *Acc. Chem. Res.,* **31,** 155-157.

92. Watanabe, K., Nakayama, T., Mottl, J., 1962. Ionization potentials of some molecules. *Journal of Quantitative Spectroscopy and Radiative Transfer,* **2,** 369-382.

93. Watts, R.J., Bottenberg, B.C., Teel, A.L., 1999. Role of reductants in the enhanced desorption and transformation of chloroaliphatic compounds by modified Fenton's reactions. *Environ. Sci. Technol.,* **33,** 3432.

94. Watts, R.J., Haller, D.R., Jones, A.P., Teel, A.L., 2000. A foundation for the risk-based treatment of gasoline-contaminated soils using modified Fenton's reactions. *J. Hazard. Mater.,* **76,** 73-89.

95. Yan, Y.E., Schwartz, F.W., 1999. Oxidative degradation and kinetics of chlorinated ethylenes by potassium permanganate. *J. Contam. Hydrol.,* **37,** 343-365.

96. Yan, Y.E., Schwartz, F.W., 2000. Kinetics and mechanisms for TCE oxidation by permanganate. *Environ. Sci. Technol.,* **34,** 2535-2541.

97. Zhang, H.B., Schwartz, F.W., 2000. Simulating the in situ oxidative treatment of chlorinated ethylenes by potassium permanganate. *Water Resour. Res.,* **36,** 3031-3042.